Ice-Associated Arctic Cod along the Chukchi Sea and Beaufort Sea Slopes during Late Fall 2019

Principal Investigator: Franz Mueter[1]

[1] College of Fisheries and Ocean Sciences, University of Alaska Fairbanks

February 2023
Final Report
OCS Study BOEM 2023-014

BOEM
Bureau of Ocean Energy Management

UAF UNIVERSITY OF ALASKA FAIRBANKS

Photo credit: John Guillote

The following individuals contributed to this report:

Hauke Flores[1], Alexei Pinchuk[2], Louise Copeman[3],
Sarah Maes[4], Maxime Geoffroy[5], Zane Chapman[2], Jared Weems[6]

[1] Alfred Wegener Institute, Bremerhaven, Germany
[2] College of Fisheries and Ocean Sciences, University of Alaska Fairbanks, Juneau, AK, USA
[3] Hatfield Marine Science Center, Alaska Fisheries Science Center, NOAA, Newport, OR, USA
[4] Catholic University of Leuven, Belgium
[5] Fisheries and Marine Institute, Memorial University, Canada
[6] Alaska Department of Fish and Game, Kodiak, AK, USA

uaf-cmi@alaska.edu
https://www.uaf.edu/cfos/research/cmi

This study was funded by the University of Alaska Coastal Marine Institute and the U.S. Department of the Interior, Bureau of Ocean Energy Management Alaska OCS Region (cooperative agreement M19AC00018). This report, BOEM 2023-014, is available electronically from https://www.boem.gov/akpubs

LIST OF FIGURES

LIST OF TABLES

ABSTRACT

Arctic cod (*Boreogadus saida*), a key forage fish for many Arctic birds and seals, may be particularly susceptible to changing sea-ice conditions because young fish utilize sea ice for shelter and feeding. This study examined to what extent young Arctic cod and their potential zooplankton prey become associated with the growing sea ice in the fall and early winter. The project leveraged ship and logistics support from the European-funded Arctic Research Icebreaker Consortium (ARICE) through a collaboration with the Alfred Wegener Institute in Germany. In November 2019, a Surface and Under-Ice Trawl (SUIT) for sampling fish and plankton was deployed from the ice-capable *R/V Sikuliaq* at the ice-water interface to sample Arctic cod and its prey. In addition, plankton samples were collected from the water column below the ice, and the ship's echosounder was used to estimate fish and zooplankton backscatter in the water column. The specific objectives of this project were to (1) support the participation of UAF faculty and students in the expedition, (2) assess the pre-winter condition of Arctic cod based on lipid analyses, and (3) assess the under-ice composition and abundance of zooplankton in late fall.

The overall project provided, for the first time, detailed information on ice-associated communities under newly formed ice in late fall. We found that Arctic cod were widely distributed along the Chukchi and Beaufort slopes at the ice-water interface and in several layers within the water column. Arctic cod were feeding on sea ice-associated zooplankton prey as well as prey in the upper water column. However, Arctic cod under the ice were in poor energetic condition, with lipid levels that are associated with high mortality rates under starvation in laboratory experiments. Thus, it is unclear if they would have been able to obtain sufficient prey to survive their first winter. Zooplankton prey was still available in moderate abundance in the water column and under the ice, which may enable Arctic cod to put on additional lipid reserves even in late November. Comparisons between summer-caught juveniles and Arctic cod sampled under the ice in November suggest that cod depleted their energy reserves between September and November 2019, possibly as a result of high water temperatures. While it has been suggested that Arctic cod may initially benefit from a warming Arctic due to an extended growing season, warmer temperatures and reduced abundances of the Arctic copepod *Calanus glacialis* may result in reduced lipid storage and ultimately compromise overwinter survival, as suggested by the poor condition of Arctic cod sampled under sea ice in this study during an unusually warm year.

INTRODUCTION

Arctic cod (*Boreogadus saida*, referred to as polar cod in the European Arctic) are the most abundant and widely distributed forage fish in the Arctic Ocean and surrounding seas, including the Pacific Arctic (Lowry and Frost, 1981; Gillispie *et al.*, 1997; De Robertis *et al.*, 2017). Because of their high abundance and energy density (Harter *et al.*, 2013), they are an important prey resource for many migrating seabirds and marine mammals (Bluhm and Gradinger, 2008) and are caught as subsistence food for humans (Magdanz *et al.*, 2010). Adult Arctic cod have a bentho-pelagic lifestyle and can reach high biomasses in some Arctic shelf and slope regions (Benoit *et al.*, 2008; Ajiad *et al.*, 2011; Geoffroy *et al.*, 2011; Boitsov *et al.*, 2013). Spawning takes place under the ice in late fall to early winter (Borkin *et al.*, 1987). The eggs float to the underside of the ice and hatch approximately 60–85 days after spawning at sub-zero temperatures (Altukhov, 1981). Developing eggs and larvae are closely associated with sea ice and may be particularly susceptible to changing ice conditions. After their first summer, postlarval Arctic cod migrate to deeper waters (Bouchard and Fortier, 2011; Geoffroy *et al.*, 2016), whereas young (1–2 years old) Arctic cod have often been observed in association with sea ice (Lønne and Gulliksen, 1989; Gradinger and Bluhm, 2004; Melnikov and Chernova, 2013; David *et al.*, 2016).

It has been proposed that at least some Arctic cod become associated with the growing sea ice in the fall, and the ice may be important for these fish both as a shelter from predators and as a foraging ground (Hop and Gjøsæter, 2013). Diet studies conducted on fish sampled in the water column or on shallow shelves during the summer suggest that Arctic cod feed mainly on pelagic copepods, amphipods, and euphausiids (Benoit *et al.*, 2010; Gray *et al.*, 2016). In contrast, the diet of Arctic cod at the ice-water interface is dominated by ice-associated ('sympagic') amphipods and copepods with a strong dependence on sea-ice algae (Kohlbach *et al.*, 2017). Sea-ice algae are a major portion of the diets of large, lipid-rich copepods, euphausiids, and sympagic amphipods in seasonally ice-covered areas (Søreide *et al.*, 2006; Wang *et al.*, 2014; Hunt *et al.*, 2016; Kohlbach *et al.*, 2016), and are important to the reproduction and growth of an ecologically important Arctic zooplankton species, *Calanus glacialis* (Søreide *et al.*, 2010; Leu *et al.*, 2011).

Our understanding of the distribution of Arctic cod and its prey is biased towards pelagic and demersal aggregations because the upper 5 m under the sea ice are inaccessible to traditional nets and sonars. Sampling of the upper 2 m of the water column under the ice with a "Surface and Under-Ice Trawl" (SUIT, van Franeker *et al.*, 2009; Flores *et al.*, 2012) demonstrated that Arctic cod were ubiquitous at the ice-water interface during summer in the Eurasian Basin of the Arctic Ocean (David *et al.*, 2016). Arctic cod have also been observed under sea ice in the Canada Basin (Gradinger and Bluhm, 2004), but the extent to which they use under-ice habitat in the Pacific Arctic is unknown. Large and dense aggregations of young-of-year Arctic cod occur on the northeast Chukchi Sea shelf (De Robertis *et al.*, 2017; Levine *et al.*, 2021), whereas the density of older (age 1+) Arctic cod on the shelf is very low (Marsh *et al.*, 2020). Although it is not known where these Arctic cod overwinter, they are likely advected via Barrow Canyon into the Beaufort Sea (Levine *et al.*, 2021), where aggregations of benthopelagic age-1 and older Arctic cod have been documented along the western (Parker-Stetter *et al.*, 2011) and eastern Beaufort Sea slope (Benoit *et al.*, 2014) during late summer and fall. Therefore, we hypothesized that at least some of these Arctic cod become associated with sea ice after its formation in late fall and early winter.

The association of juvenile Arctic cod with under-ice habitat and their apparent dependence on ice algal carbon (Kohlbach *et al*., 2016) suggests that the entrainment of young Arctic cod to sea-ice habitat during fall may be an important process in a sea ice-associated survival strategy. However, this hypothesis has

not been tested to date. Our understanding of the relationships between sea-ice habitats, environmental conditions, phytoplankton, sympagic fauna, and zooplankton community structure in the Arctic Ocean, and its impacts on higher trophic levels, including humans, remains very limited (Bluhm et al. 2015). Progress to date has been limited by the logistical challenges of sampling fish and their prey under the ice. Therefore, to better understand the importance of sea ice for Arctic cod and to help resolve their life history in the Pacific Arctic system, we used a SUIT deployed from the ice-capable *R/V Sikuliaq* to sample fish and zooplankton along the advancing ice edge off Alaska in fall 2019 as part of project *Go-West: Sea-ice association of Arctic cod and its prey in the western Arctic Ocean* with ship time for sampling Arctic cod provided by the Arctic Research Icebreaker Consortium (ARICE). The cruise included Arctic cod sampling from along the ice-water interface, vertical zooplankton sampling of the upper 100 m, high-resolution profiling of sea-ice properties, and hydroacoustic profiling of the water column. The current project uses the data acquired during the Go-West project to examine the under-ice distribution of Arctic cod, their diet and conditions, and potential prey in relation to sea-ice habitat properties in the Pacific Arctic.

The overall goal of the Go-West project was to test the hypothesis that the entrainment of young Arctic cod into the sea-ice habitat in the Chukchi and Beaufort seas during the fall is significant and that the sea ice provides suitable habitat for overwinter survival. Specifically, we (1) quantified the distribution of Arctic cod and other ice-associated fauna relative to habitat characteristics using the SUIT, (2) assessed the diet composition of ice-associated Arctic cod through metabarcoding and visual analyses of stomach contents, (3) assessed the pre-winter condition of Arctic cod through lipid analyses, and (4) tested for the presence of scattering layers in the underlying water column using the ship's EK80 echo sounder. In addition, this project provided support for a graduate student to determine the daily ages of larval and juvenile Arctic cod collected in the Chukchi and Beaufort seas.

METHODS

Study Area

Our study area encompassed the marginal ice zones in the Beaufort and Chukchi seas at a time when sea-ice formation and potential entrainment of juvenile Arctic cod are occurring (Figure 1). Our goal was to sample transects across the ice edge from open water into consolidated first-year ice. Actual sampling locations were selected based on the position of the ice edge during the time available for sampling and general ice conditions in the area. The eastern Chukchi Sea and the western Beaufort Sea were selected because of known late summer aggregations of juvenile Arctic cod in the Northeast Chukchi Sea, from where they are advected into this area with the prevailing currents (Levine *et al.*, 2021). Aggregations of age-0 and older Arctic cod have previously been observed along the Beaufort Sea slope (Parker-Stetter *et al.*, 2011; Benoit *et al.*, 2014; Geoffroy *et al.*, 2016). The ice edge during much of the cruise coincided approximately with the outer shelf and upper slope regions, although much of the Beaufort Sea shelf in the eastern part of the study region was covered by ice near the mid-point of the cruise (Figure 1B). Our goal during the cruise was to sample stations along cross-shelf transects from the outer shelf/upper slope to the lower slope/Arctic basin. Ice conditions were highly dynamic during the cruise as the ice edge was rapidly advancing.

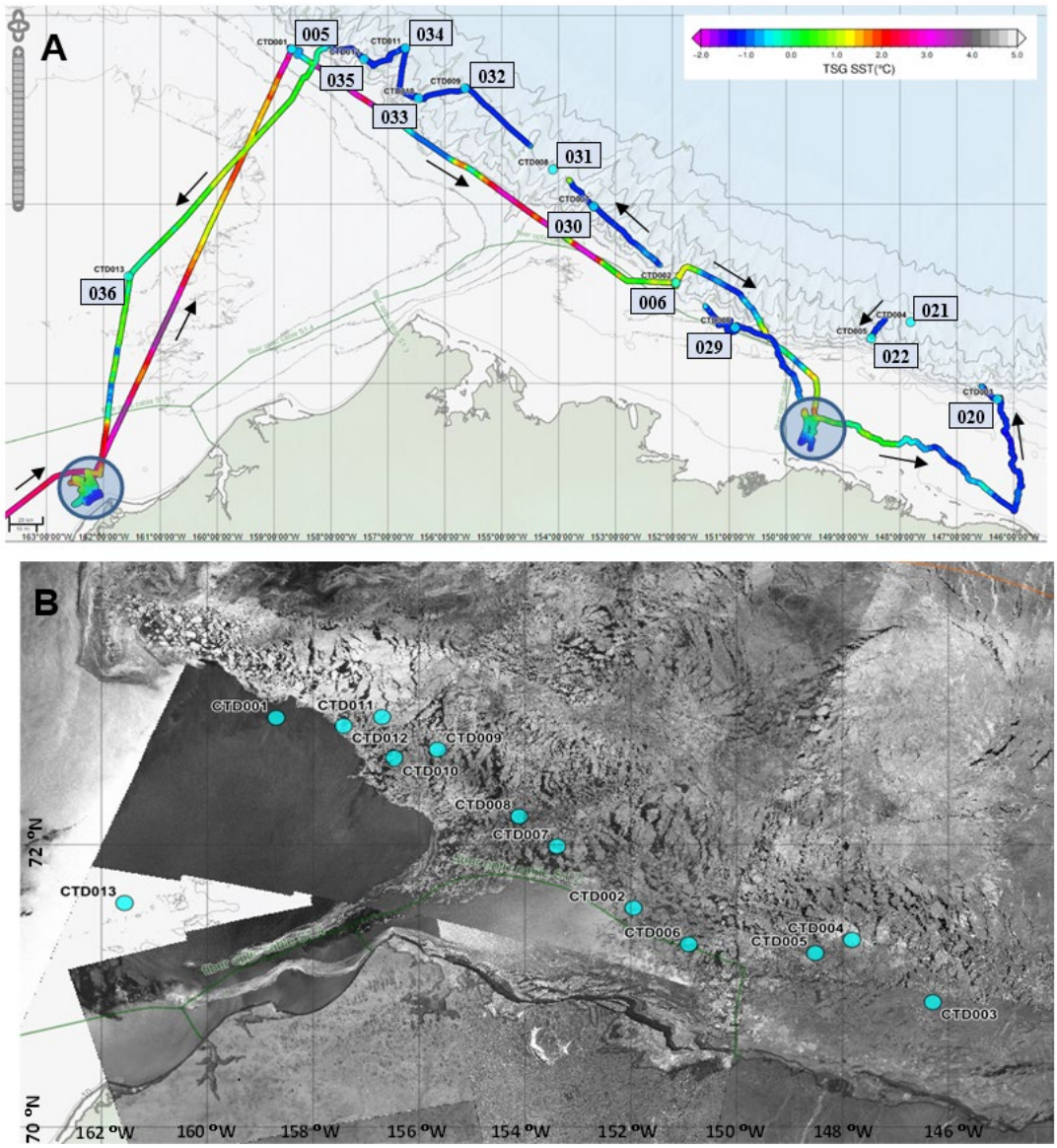

Figure 1: (A) Cruise track sampled during Go-West Cruise, November 9–22, 2019 with underway sea-surface temperatures (SST). Light-blue circles denote CTD sampling locations with main station numbers indicated in boxes. Arrows indicate direction of travel. Gaps in the SST record indicate heavier ice conditions when underway water intake was suspended. Large circles denote areas where nearshore work was conducted by the CODA project. Stations 005 and 036 denote ONR mooring site and the Chukchi Ecosystem Observatory, respectively. (B) SAR images of sea-ice cover on November 17, 2019, based on RADARSAT-2 (Canadian Space Agency) and Sentinel-1 (European Space Agency) images.

Field Sampling

A total of 13 stations were occupied between November 10 and November 20, 2019 (Table 1). At full sampling stations, we deployed the ship's CTD and rosette water sampler, a CalVET zooplankton net, the Surface and Under-Ice Trawl (SUIT), and a midwater trawl (Methot or IKMT trawl). A ring net (150 µm) was deployed at selected stations to collect live zooplankton for respirometry. In addition to the fisheries stations, we obtained two opportunistic CTD/oceanography stations at the site of an Office of Naval

Research (ONR) acoustics mooring along the Chukchi Slope (Station 005, Figure 1) and at the site of the UAF long-term Chukchi Ecosystem Observatory (Station 036, Figure 1).

Ice conditions throughout the period when the ship was operating in or near the ice were characterized based on hourly ice observations conducted from the ship's bridge. Ice concentration (%) and ice type were classified following the ASSIST (Arctic Ship-based Sea Ice Standardization) and ASPeCt (Antarctic Sea-Ice Processes and Climate) protocols (e.g., Zong *et al.*, 2022). Additional environmental data were obtained from the ship's data archive, including underway data and available SAR images of ice cover during the cruise from RADARSAT-2 (Canadian Space Agency) and Sentinel-1 (European Space Agency). Underway data relevant to the project were collected along much of the cruise track and included bottom depth from the ship's EM302 sounder, temperature and salinity below the surface at 4 m from the ship's thermosalinograph, Photosynthetically Active Radiation (PAR) from the ship's radiometer, and wind speed and direction.

Table 1: Fishing and oceanography stations sampled by the GO-WEST project during November 2019.

Station	Date (local)	Depth	CTD	CalVET Net	Ring Net	SUIT	Methot Net	IKMT	Ice Station
005[a]	10-Nov	303	001		X				
006[b]	11-Nov	760	002	X		X[c]	X		
020	14-Nov	169	003	X	X	X	X[e]		
021	15-Nov	2382	004	X	X	X[c]		X	X
022	15-Nov	1286	005	X		X			
029	17-Nov	200	006	X	X	X			X
030	18-Nov	1550	007	X	X	X[c]			X
031	18-Nov	1894	008	X		X			
032	19-Nov	2550	009	X	X	X[d]			
033	19-Nov	1553	010	X		X[c]			
034	19-Nov	2059	011	X		X			
035	20-Nov	986	012	X	X	X			
036[f]	20-Nov	48	013	X					

[a] ONR mooring site (trial CTD and filtration); [b] Open water SUIT trial; [c] One aborted attempt; [d] Two aborted attempts; [e] Methot net frame badly damaged; [f] Chukchi Ecosystem Monitoring (CEO) mooring site

Oceanographic sampling was conducted with the shipboard CTD Rosette (Seabird 911 CTD/sensor package and 24 x 12L Niskin bottles). Casts were conducted at each station to 300 m depth or 3–5 meters from the seafloor at shallower locations. CTD sensor data were recorded throughout the cast and were processed immediately upon recovery. Water samples were taken by Niskin bottle at 300 m or near the bottom and in selected depth strata during the upcast corresponding to the secondary chlorophyll maximum (as determined during the downcast), just below the pycnocline, at the chlorophyll maximum, and at the surface (3–5 m). Water samples were filtered and preserved following the NOAA-AFSC-FOCI

protocols for later laboratory analysis of nutrients, chlorophyll *a* (Chl*a*), and phytoplankton species composition. Nutrient samples were filtered immediately upon retrieval of the CTD Rosette using a syringe. For measuring Chl*a*, two 500 ml bottles of water were collected from each sampling depth and were immediately filtered in a cold laboratory under low light through a Whatman GF/F filter (nominal pore size 0.7 µm) and then polycarbonate filters (pore size 5 µm) to estimate total and size-fractionated (> 5µm) Chl*a*. Water samples (250 ml) from the chlorophyll maximum layer were preserved in 10% buffered formalin for analysis of phytoplankton species composition. Surface water samples (125 ml) were preserved in Lugol solution for microscopic analyses of harmful algae. Two samples per station (500 ml water each) were filtered for biomarker analysis of Particulate Organic Matter (POM) using GF/F filters, and one sample (2 L) was filtered for eDNA analyses using 0.2µm filters. After filtration, all filters were stored in separate vials at -80°C.

Mesozooplankton was sampled at most stations with a 25-cm diameter CalVET system (CalCOFI Vertical Egg Tow) with two 150-µm mesh nets (Table 1). The nets were fished vertically from approximately 100 m depth to the surface and were equipped with General Oceanics flowmeters in the mouth of the net. The estimated volume filtered ranged from 35.9 to 53.6 m^3. Volumes recorded from the flowmeter were compared with volumes estimated from the distance (depth) towed at each station to detect potential net clogging. In practice, little clogging occurred, and the nets performed with nearly 100 % filtration efficiency. All samples were immediately preserved in a 10% formalin/borax/sea water solution for later sorting.

Macrozooplankton and fish were sampled at the ice-water interface using the SUIT and throughout the upper 100-200 m using a midwater trawl (Methot or IKMT). The SUIT was equipped with a fish net with a mesh size of 7 mm and a mesozooplankton net with a mesh size of 300 µm. The SUIT was successfully deployed at 11 stations, but ice conditions prevented us from sampling the water column with a midwater trawl at all but 3 of those stations (Table 1). The SUIT was towed over distances of 815 to 2201 m at mean speeds between 0.59 and 1.27 m sec^{-1} and under ice between 11 and 51 cm. The contents of both nets were rinsed down into the codend and were processed on board for further analysis (see below). Both nets, but in particular the zooplankton net, occasionally collected large amounts of ice that filled up to about one-third of the smaller mesh net. Video footage from a camera mounted inside the SUIT frame suggested that ice crystals floating in the water column below the sea ice were collected in the net along with organisms. Macrozooplankton catches from these tows were not considered quantitative as the ice likely affected the performance of the net.

In addition to zooplankton and fish, environmental data were collected along the length of the tow using environmental sensors attached inside the SUIT. Sensors included an altimeter (Tritech PA500) to measure distance to ice, a hyperspectral sensor (RAMSES, TRiOS) to measure optical properties of the ice during daytime hauls, a CTD (RBRbrevio3) to measure depth, temperature, salinity, and chlorophyll *a* concentration, and an Acoustic Doppler Current Profiler (ADCP, Nortek Aquadopp) to measure speed through the water and the estimated volume filtered. Ice draft was estimated from the depth measured by the CTD's pressure sensor and the distance of the SUIT to the ice derived from altimeter data. Sea-ice draft was converted to ice thickness by multiplying the ice draft by the ratio of the density of surface water to the density of sea ice. Seawater density was calculated from measured surface temperature and salinity and sea-ice density was assumed to be 0.91 kg/l, the approximate average density of first-year ice (Timco and Frederking, 1996).

Live zooplankton were collected opportunistically at 7 stations during the cruise (Table 1) using a ring net (0.5m diameter, 150 µm mesh size) for onboard experiments with a respirometer to measure their oxygen consumption at ambient water temperatures. The ring net was hauled vertically from 50 m depth or, at shallower stations, from near the sea floor to the surface. The ring net was deployed twice to increase the sample size of zooplankton organisms per station.

Finally, to obtain estimates of acoustic backscatter from zooplankton and fish in the upper 300 m of the water column, the ship's EK80 was deployed continuously throughout the cruise during light ice conditions and while traveling in open water deeper than 20 m. The EK80 unit was housed in the centerboard, which was put in a flush position or retracted during heavier ice conditions, resulting in some gaps in the acoustic record. We collected narrowband acoustic data at 18, 38, 70, 120, and 200 kHz with a ping rate of 1 Hz and a pulse length of 1.024 ms(p). The echosounder was calibrated using the standard sphere method (Demer *et al.*, 2015) before the survey in August 2019. On 15–16, November acoustic data were only recorded to a depth of 312 m. Screenshots of acoustic backscatter at 18, 38, 70, 120, and 200 kHz were taken every 30 min and archived for visual inspection.

On-board Sample Processing and Experiments

Zooplankton

Macrozooplankton caught in the SUIT net were immediately identified to the lowest taxonomic level possible and counted. Macrozooplankton specimens were stored frozen for later analysis. Selected zooplankton species including *Clione limacina* and *Gammarus wilkitzkii* were sampled for trophic biomarker analysis and stored at -80°C. Mesozooplankton from the SUIT's 300 µm mesh net was preserved in formaldehyde for later taxonomic analysis. Abundant samples were split with a folsom zooplankton splitter, and 50% of the catch was size-fractionated (2000, 500, 150 µm) and stored in Petri dishes at -20°C.

Fish

We successfully captured fish at the ice-water interface and in the water column using the SUIT and two midwater trawls. A total of 170 juvenile Arctic cod (as identified in the field), ranging from 1 to 38 fish per station were captured and processed. Most fish were measured (Total Length, TL), weighed, and processed for subsampling of tissue samples immediately after retrieval. Tissue samples from Arctic cod included fin clips for population genetic analyses, stomachs for diet analysis, hind guts for microbiome analysis, muscle tissue for trophic biomarker analysis, and otoliths for age determination.

Respirometry experiments

Zooplankton caught with the ring net were pre-sorted according to condition, species, and stage in a temperature-controlled room (3-5°C) and briefly stored in filtered seawater (GFF filter, 25 mm). The individuals then were transferred into a sensor dish plate (PreSens, Regensburg, Germany) comprising 24 compartments (wells) for the measurement of individual respiration. Up to 20 specimens were placed in the respiration setup, while at least four wells remained empty for the detection of bacterial respiration. The wells were filled with pre-aerated filtered station water at -1.0°C right before sealing. After sealing, the plate was submerged in a glycol solution in a flow-through chamber connected to a Polystat pump chiller (Cole-Parmer, Vernon Hills, IL), and the assembly was placed on top of a sensor dish reader (PreSens, Regensburg, Germany). The measurement temperature was maintained at -1.0°C (except during preliminary trials). All respiration measurements were performed in the dark and lasted for 13–25 h. In

these on-board experiments, we focused predominately on juvenile *Calanus glacialis* (Stages IV and V) and *Metridia longa* (stage V juveniles and adult females), because these species' appeared to be most dominant in the water column by biomass. In addition, preliminary experiments showed that a body length of approximately 5 mm was most suitable for the detection of a respiratory signal in a water body of 1.6 ml volume.

Laboratory Processing and Analyses

Nutrients and chlorophyll a

Frozen samples collected during the cruise were analyzed for nutrients (phosphorus, silicic acid, nitrate, nitrite, ammonium) at NOAA's Pacific Marine Environmental Laboratory following WOCE-JGOFS standardization and analysis procedures specified by Gordon *et al*. (1993), including calibration of labware, preparation of primary and secondary standards, and corrections for blanks and refractive index. In this method, nitrate + nitrite and nitrite are both measured, and nitrate is determined from the difference. Ammonium was measured using an indophenol blue method modified from Mantoura and Woodward (1983). Frozen (-80°C) chlorophyll filters were analyzed at NOAA's Pacific Marine Environmental Laboratory with a Turner Designs (TD-700) bench-top fluorometer following standard methods (Parsons *et al.*, 1984).

Zooplankton

Preserved zooplankton samples were split sequentially in the laboratory using a Folsom splitter until the smallest subsample contained about 200 specimens of the most abundant taxa. The most abundant taxa were identified, staged, counted, and weighed. Each larger subsample was examined to identify, count, and weigh the larger, less abundant taxa. Blotted preserved individual wet masses were determined for larger taxa, while individual wet masses obtained from earlier studies in the Western Arctic (Coyle and Pinchuk, 2002; Pinchuk and Eisner, 2017) were used to calculate the biomass of small (<2 mm) taxa.

Arctic cod population structure

Smaller fish for which morphological identification was inconclusive were molecularly identified with DNA barcoding following the protocol described in Bouchard et al. (2020). In brief, DNA was extracted and the primers FishCOILBC and FishCOIHBC-deg ((Handy *et al.*, 2011)) were used to amplify a fragment of the mitochondrial cytochrome oxidase subunit I (COI) gene. After standard sequencing, the obtained COI sequences were matched to the Barcode of Life Data system (BOLD; Ratnasingham and Hebert, 2007) to identify whether the queried individuals were Arctic cod, polar cod (*Arctogadus glacialis*), or other fish.

Genetic analyses of population structure were conducted at a circumpolar scale that included a total of 367 Arctic cod from 15 regions in the Arctic Ocean collected between 2012 and 2020, including 52 specimens from the Alaskan Arctic collected during this study (Maes 2022). Fin clips were taken and stored at 96% ethanol for analysis at the Catholic University of Leuven (KUL). Juvenile fish were identified morphologically by experts onboard. Larvae and small juveniles were molecularly identified in the laboratory with DNA barcoding of the mitochondrial COI gene. Samples were processed and analyzed as detailed in Maes (2022).

Arctic cod diets and gut microbiomes

Diet compositions of Arctic cod were examined using visual analyses of stomach contents and DNA metabarcoding. All stomachs were examined for stomach fullness. For visual analyses, stomach contents

were gently removed from 22 Arctic cod stomachs, and ingested prey items were visually examined under a microscope. Prey items were identified to the lowest taxonomic level and developmental stage possible. The degree of digestion of prey was recorded according to the following scale: (1) fresh prey, (2) slightly digested prey, (3) well-digested prey, and (4) severely digested barely identifiable prey. Total prey wet mass was determined by multiplying a mean individual prey taxon wet mass, obtained from zooplankton data by the number of that specific prey taxon in the gut.

For genetic analyses of diet composition, stomach contents were homogenized, and DNA was extracted using the NucleoSpin® Tissue kit (Macherey-Nagel) following the manufacturer's instructions. Analyses were conducted by collaborators at the Catholic University of Leuven (KUL), Belgium. Because stomachs were small, the entire stomach content was extracted without subsampling. The DNA metabarcoding library was prepared according to the protocol described by Maes et al. (2022). The data were processed to create amplicon sequence variants (ASVs) that resolve differences in sequence variants up to one single nucleotide (Callahan *et al.*, 2017)). The following criteria were used for taxonomic assignment in the Barcode of Life Database (BOLD): (1) a taxon was assigned if the barcode matched a single locally occurring taxon in the databases with ≥ 97 % sequence similarity level; (2) in case the barcode matched more than one taxon with ≥ 97 % sequence similarity level, a taxon was assigned at the genus-level. Species that were highly likely identified as within-laboratory contaminations (i.e., study species from the home laboratory) were excluded. Taxa seen at least twice in at least 1% of the samples were retained and samples with less than 20 reads in total were discarded. Sequence reads were analyzed based the on frequency of occurrence (% FOO, i.e., presence/absence of taxa) and relative read abundance (% RRA). Frequency of occurrence was estimated as the proportion of individuals containing a particular prey taxon.

Finally, the gut microbial diversity of Arctic cod collected in the Pacific Arctic was examined by collaborators at KUL to establish an ecological baseline of the bacterial diversity of the Arctic cod gut microbiome. The composition of the gut microbial community was determined with 16S rRNA metabarcoding for 90 juvenile Arctic cod sampled under sea ice in the Beaufort and Chukchi Seas. The gut microbiome was compared to that of 25 Arctic cod from the Barents Sea sampled during summer in open water. Details of the analysis are described in Maes (2022).

Lipid analyses

Analyses of lipid classes on Arctic cod were conducted at the Marine Lipids Laboratory at the Hatfield Marine Science Center in Newport, OR, USA. Tissues were homogenized in chloroform and methanol and total lipids were extracted according to Parrish (1987) using a modified Folch procedure (Folch *et al.*, 1957). Total lipids and lipid classes were determined using thin-layer chromatography with flame ionization detection (TLC/FID) with a MARK V Iatroscan (Iatron Laboratories, Tokyo, Japan) as described by Lu *et al*. (2008). Detailed procedures for lipid class analyses of juvenile gadids are described in Copeman *et al*. (2016, 2017).

Otolith analyses

Otoliths from the cruise have been preserved for aging but have not been analyzed yet. Some otoliths were examined for daily growth increments but were too large for daily aging. However, archived otoliths of larval and juvenile Arctic cod from other cruises in the Beaufort Sea and Chukchi Sea were used to determine hatch dates of young-of-year Arctic cod sampled in late summer as detailed in Chapman et al. (2023).

Acoustic Data Processing

Acoustic data were visually scrutinized and cleaned using the Echoview v.10 software. Profiles of temperature and salinity taken at sampling stations were averaged daily to correct the coefficients of absorption and sound speed. Because of the ship's draft and near-field regions, the top 10 m (38, 70, 120, 200 kHz) or 25 m (18 kHz) were removed from the analysis. The first meter above the seafloor was also discarded because of the dead zone (Simmonds and MacLenna, 2006). Impulse and attenuated noise were detected and removed using the algorithms described in Ryan *et al*. (2015). Background noise was removed using a signal-to-noise ratio (SNR) threshold of 10 dB (De Robertis and Higginbottom, 2007). We echo-integrated and exported the volume backscattering strength (S_v in dB re $1m^2\,m^{-3}$) at each frequency with a resolution of 0.25 nautical miles by 3 m depth. Due to decreasing SNR with range and frequency, the signal was exported down to 500 m at 18, 38, and 70 kHz, and down to 300 m at 120 and 200 kHz.

The average profile of backscatter at each frequency was calculated and a Gaussian kernel smoothing with a vertical resolution of 25 m was applied using the library 'smoother' in R. We calculated the integrated area-backscattering strength (S_a in dB re $m^2\,m^{-2}$, an index of abundance), center of mass (CM), and index of aggregation (IA, a measure of patchiness) based on the equations in Urmy *et al*. (2012). All calculations were conducted in the linear domain before being log-transformed (dB). Target Strength frequency distributions were exported using the variable 'Single target detection - Split Beam Method 2' in Echoview.

Statistical Analysis

To explore spatial patterns in the abundance of Arctic cod, we conducted simple correlation and regression analyses. Counts of Arctic cod were standardized as Catch-Per-Unit-Effort (CPUE) based on the volume filtered by the SUIT for mapping and correlation analyses. Due to the small number of stations sampled (n=11) and the skewed distribution of CPUE, we modeled counts as a function of individual explanatory variables using a negative binomial regression using raw counts with effort as an offset in the model (Zuur *et al.*, 2012). Explanatory variables considered in these analyses include bottom depth (shelf break/slope bathymetry), ice thickness (a proxy for age), surface layer salinity (Mackenzie River influence), light conditions (day, night, twilight), and surface chlorophyll concentration. Additional exploratory correlation analyses were conducted to assess possible relationships between Arctic cod abundance and other potential covariates, including the abundance of individual zooplankton taxa.

To describe genetic variability within and across Arctic cod populations, standard indices of genetic diversity such as observed and expected heterozygosity and inbreeding coefficients were calculated for each putative population. To measure the genetic differentiation between putative populations, pairwise F_{ST} values were computed and evaluated for significance. A hierarchical analysis of molecular variance (AMOVA) was performed to detect population differentiation. Principal Component Analysis (PCA), Discriminant Analysis of Principal Components (DAPC; Jombart *et al.*, 2010), and STRUCTURE analysis (Pritchard *et al.*, 2000) were used for clustering Arctic cod individuals to understand population groupings across the Arctic. A detailed description of the methods is provided in Maes (2022).

RESULTS

The GO-WEST project successfully occupied a total of 11 fishing stations and two additional oceanography stations (Table 1). We describe oceanographic characteristics including nutrients and chlorophyll *a*, zooplankton abundances, the abundance and distribution of Arctic cod from net samples

and acoustics, their diet composition, and their energetic condition. Physical, chemical, and biological properties were examined for spatial patterns along the Chukchi and Beaufort Sea slopes and relative to potential explanatory variables.

Water Column Characteristics

Surface waters along the shelf break and slope were below 1°C except off the mouth of Barrow Canyon on the outbound track, where surface temperatures ranged up to 3.5°C (Figure 1, Appendix 1). When operating in or near sea ice, surface temperatures were typically between -1.5 and 0°C. The water column structure at most stations was characterized by highly stratified water masses with very similar surface and deep waters across the region but considerable differences at intermediate densities (Figure 2).

Surface waters (~0–30 m) had low temperatures (0 to -1.5°C) and low salinities (27–29) due to strong atmospheric cooling at the surface before and during the cruise and relatively high freshwater runoff in the region (Appendix 1, Figure A 1). Eastern Beaufort Sea surface waters were especially cold and had the thickest, oldest sea ice by mid-November (Figure 1B). Below the pycnocline (20c35 m), remnants of warmer waters from the summer with significant heat content remained at depths of about 30–70 m, particularly in the western part of the region and downstream from Barrow Canyon (Figure 3). This summer layer was characterized by warmer but highly variable temperatures (1–4°C) and elevated salinities (30–32). Below this warmer layer, a cold (<0°C), more saline (31–33) mixed Arctic water layer extended down to ~200m depth, overlaying a warmer (>0°C), highly saline (33–34) layer of Atlantic deep water that impinges on the Chukchi and Beaufort slopes.

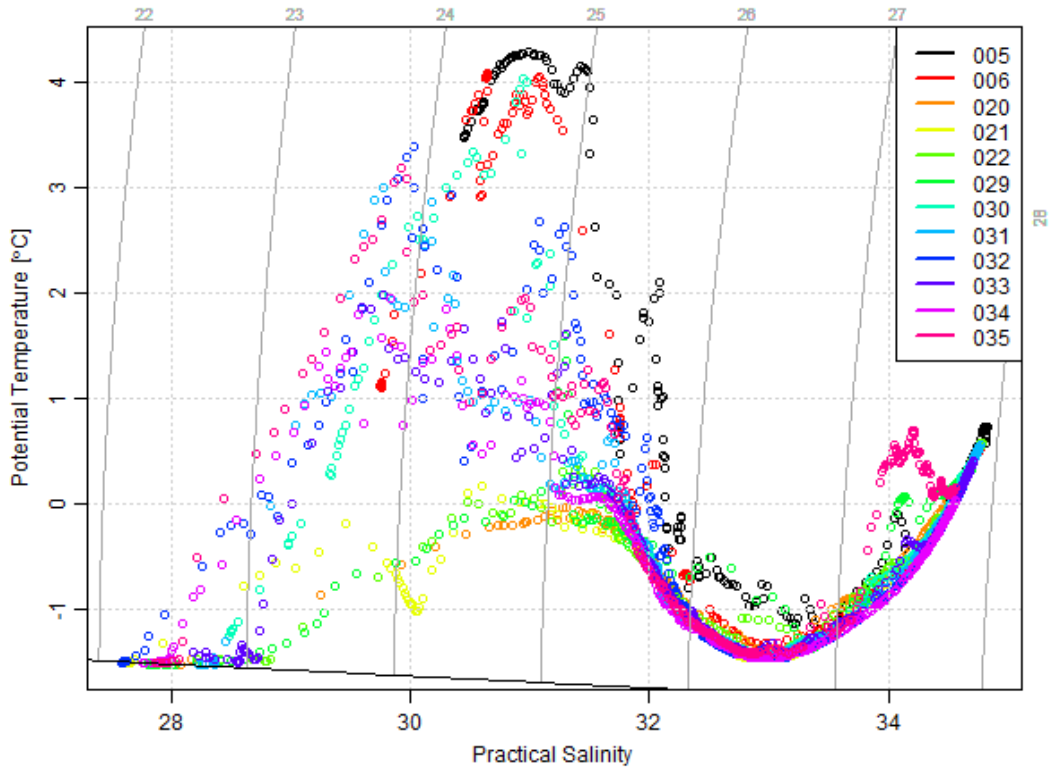

Figure 2: Temperature-salinity plots for all CTD stations occupied in the marginal ice zone along the Chukchi and Beaufort Sea slope regions in November 2019. See Figure 1 for station locations.

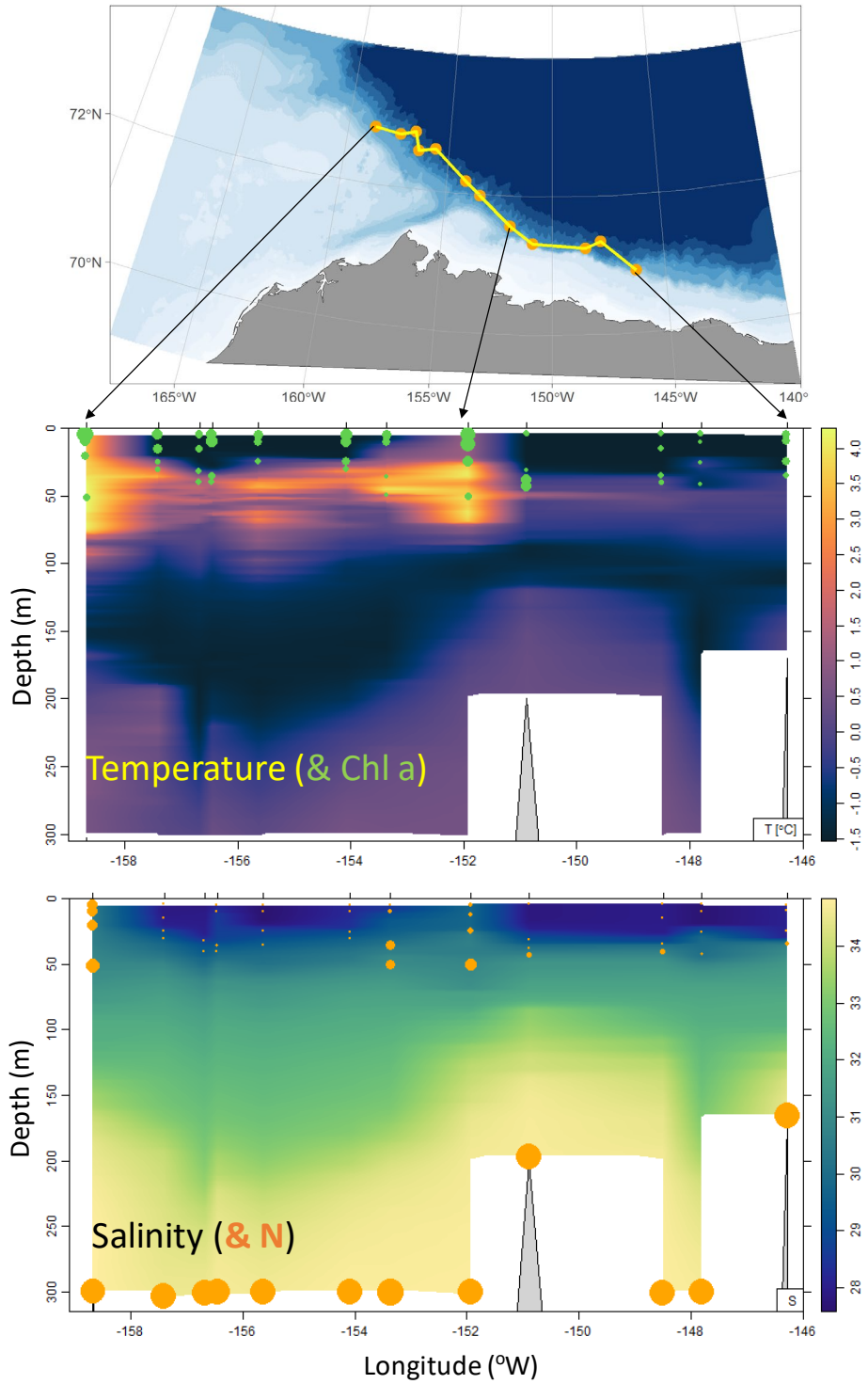

Figure 3: Temperature, salinity, chlorophyll *a* and total nitrogen results from the study area. Temperature and salinity were taken on transects along the Chukchi and Beaufort slopes from west to east as depicted in the map at the top. Chlorophyll *a* concentration and total nitrogen (nitrate + nitrite + ammonium) from bottle data are superimposed on the temperature and salinity plots. Circle sizes are proportional to concentrations with a maximum of 0.29 µg/L and 14.1 µM, respectively.

Nutrients and Chlorophyll

Despite very low light levels in November, moderate production appeared to be occurring in the surface layer as evident in chlorophyll concentrations up to 0.25 mg m^{-3} at some stations, particularly those just outside the ice in the western Chukchi Sea and off Barrow Canyon (Figure 4). Nutrients in the surface layer were generally low along the slope and intermediate (5–6 µM) on the Chukchi shelf (Figure 4) but ranged from 12 to 15 µM at depth (300 m). While the highest Chl*a* levels were observed near the surface, concentrations up to 0.20 µg/L were observed throughout the water column (Figure 5). The highest surface concentrations were associated with the warmest water temperatures (i.e., stations outside the ice), whereas Chl*a* concentrations below the surface did not show any apparent relationship with temperature. Elevated nutrient levels were also observed below 30 m at two stations off the mouth of Barrow Canyon.

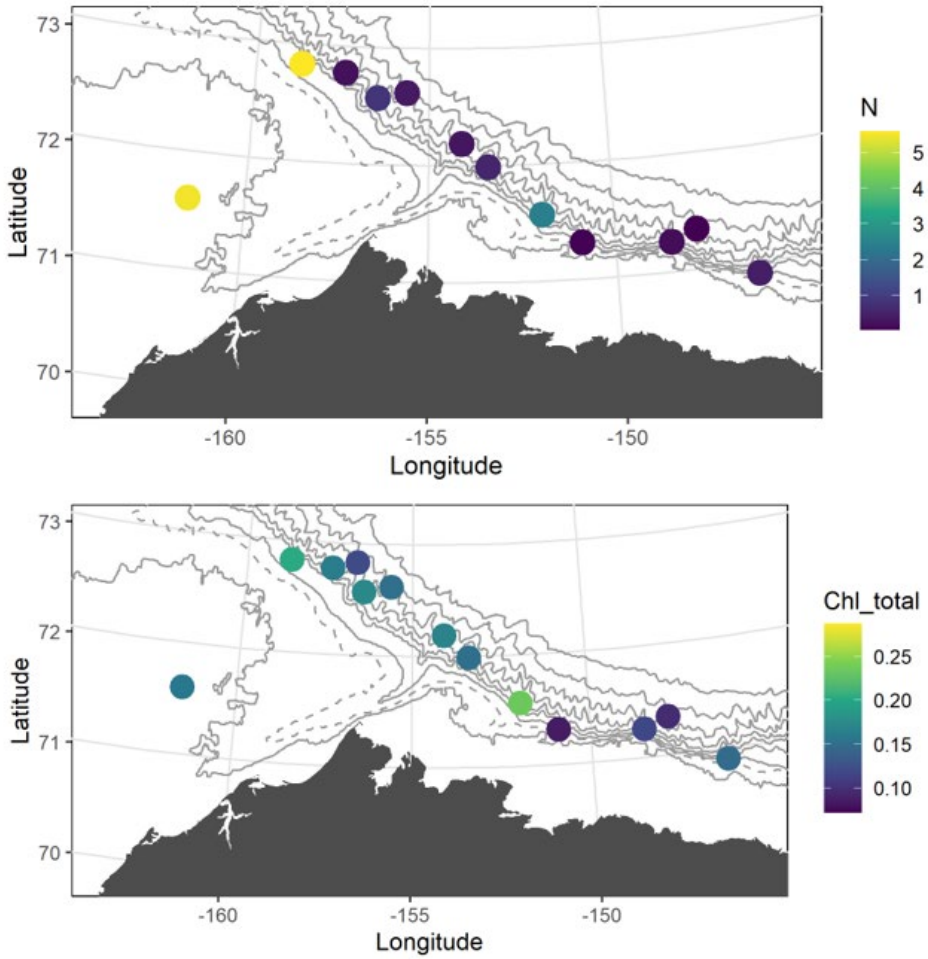

Figure 4: Total surface nitrogen (nitrate + nitrite + ammonium) and total surface chlorophyll *a* concentrations at 13 oceanographic stations sampled in the Chukchi and Beaufort seas in November 2019.

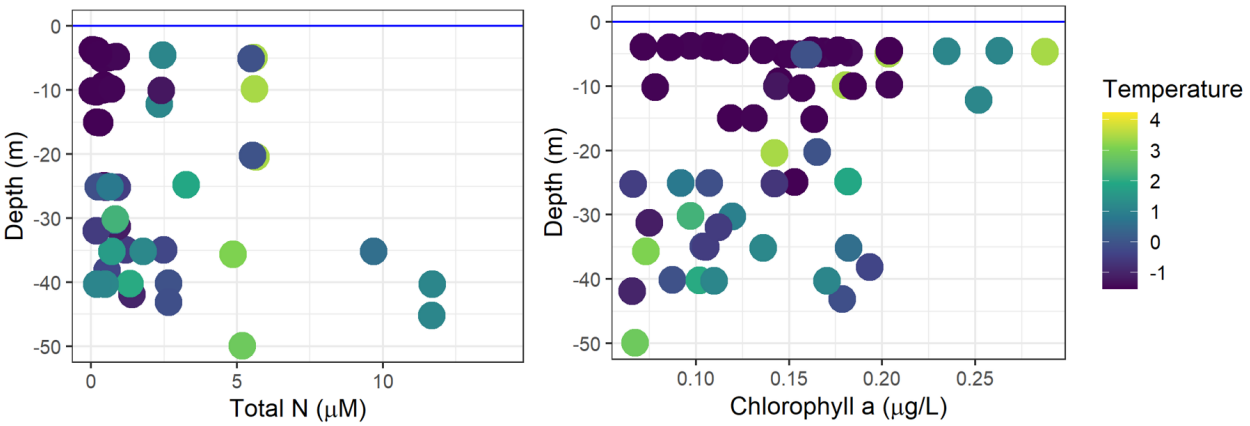

Figure 5: Total nitrogen (nitrate + nitrite + ammonium) and total chlorophyll *a* concentration by depth at 13 stations sampled in the Chukchi and Beaufort seas in November 2019. Samples were taken at selected depths (surface, pycnocline, primary and secondary chlorophyll maxima) so concentrations are not representative of the entire water column. Nutrients at 300 m (not shown) ranged from 12–15 μM.

Zooplankton

A total of 34 unique zooplankton taxa were recorded from CalVET tows sampling the upper 100 m of the water column. Zooplankton abundance was low at most stations (mean 70 individuals m^{-3}) except at the only ice-free station (006) sampled to the east of Barrow Canyon at the beginning of the cruise (Figure 6). Small (<2 mm total length) boreal neritic copepods, particularly *Oithona similis*, *Pseudocalanus* spp., and *Microcalanus* spp. were numerically dominant at all stations and comprised over 75 % of the zooplankton community by number. In contrast, large (>2 mm total length) Arctic copepods *Calanus hyperboreus*, *Paraeuchaeta glacialis*, and *Metridia longa*, and chaetognaths *Parasagitta elegans* comprised the bulk of the zooplankton biomass at all stations (mean 91 mg m^{-3}) (Figure 6). Arctic copepods *Chiridius obtusifrons* and *Heterorhabdus norvegicus* occurred in small numbers at deep stations indicating the potential influence of deep Atlantic water. Ostracods (likely *Boroecia maxima*) were recorded in all tows albeit in small quantities.

Larger zooplankton were captured in the SUIT macrozooplankton net, both in open water (station 006) and at 11 stations under the sea ice (Figure 7). Because the net frequently filled up with ice, density estimates for macrozooplankton are not considered reliable. Nevertheless, several patterns emerged that suggest spatial differences in abundance and species composition. Apparent abundances were typically lower along the Beaufort Slope stations (stations 20–29) and higher along the Chukchi Slope (stations 32–35). Moreover, the former had higher abundances of *Gammarus wilkitzkii*, while the latter were dominated by *Clione limacina* and, in some cases, by the mysid *Neomysis rayii*, which lives in coastal waters and is not known to be associated with under-ice habitat.

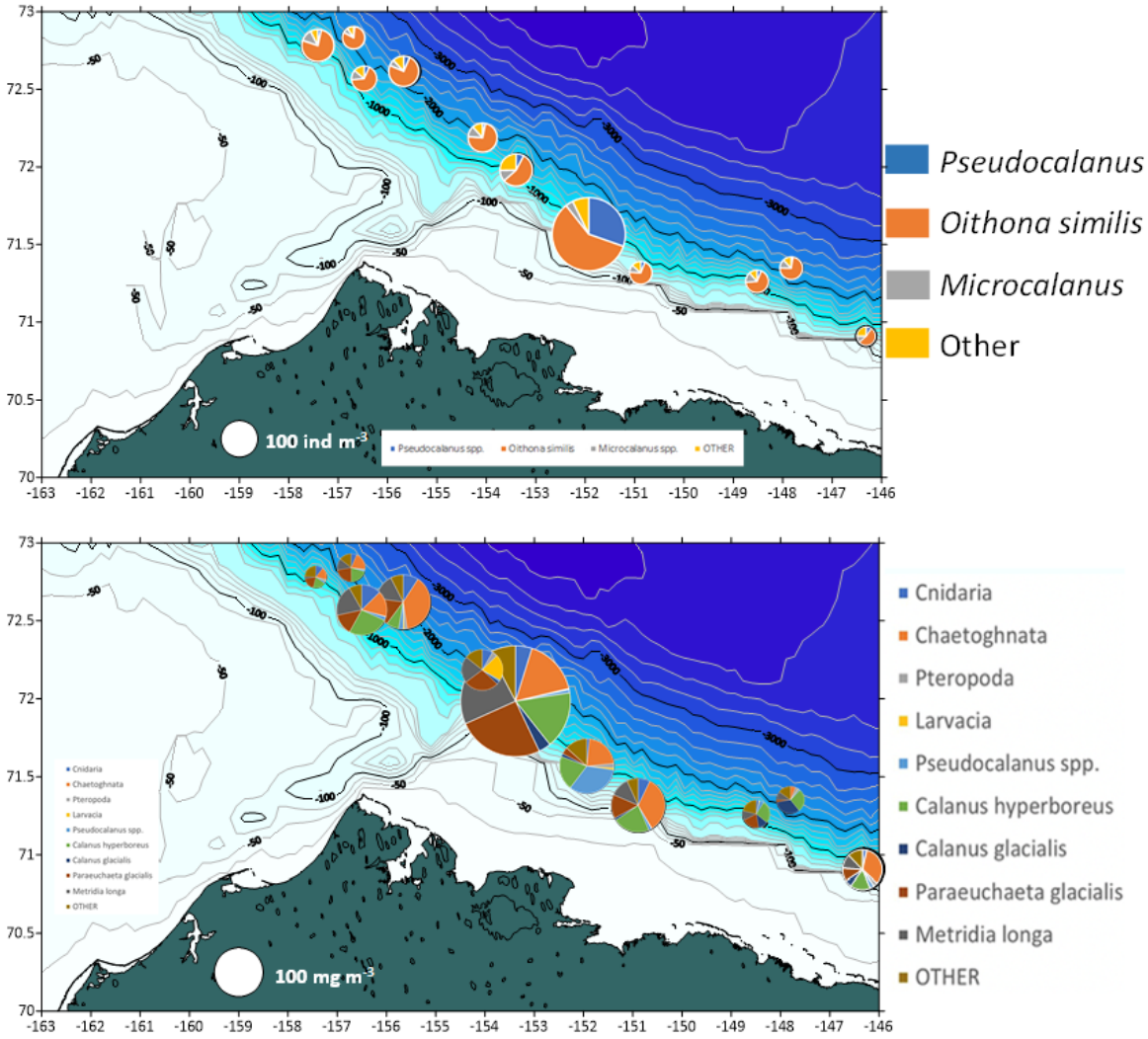

Figure 6: Abundance (individuals / m^3, top) and biomass (mg/m^3, bottom) of mesozooplankton species (150 µm mesh net) at 12 stations sampled along the Chukchi Sea and Beaufort Sea slopes in November 2019. Pies denote proportions by species.

The only station sampled with the SUIT in open water, just outside the advancing ice, had a very different mix of species with high densities of *Themisto* spp. and hyperiid amphipods. These species were absent from most ice-covered stations (Figure 7). The species composition of the two Methot trawls (0–200 m) differed markedly from the SUIT samples and between the open water station in the western Beaufort Sea (006) and a shallower station in sea ice in the eastern Beaufort Sea (020, Figure 1). At the open water station, *Themisto* spp. were abundant at the surface (SUIT) and in the midwater (Methot). However, unlike the surface sample, the midwater community was dominated by krill (*Thysanoessa raschii* and T. *inermis*). While the ice-covered station also had some krill (both *T. raschii* and *T. inermis*), large zooplankton in the midwater were numerically dominated by amphipods and *Clione limacina*.

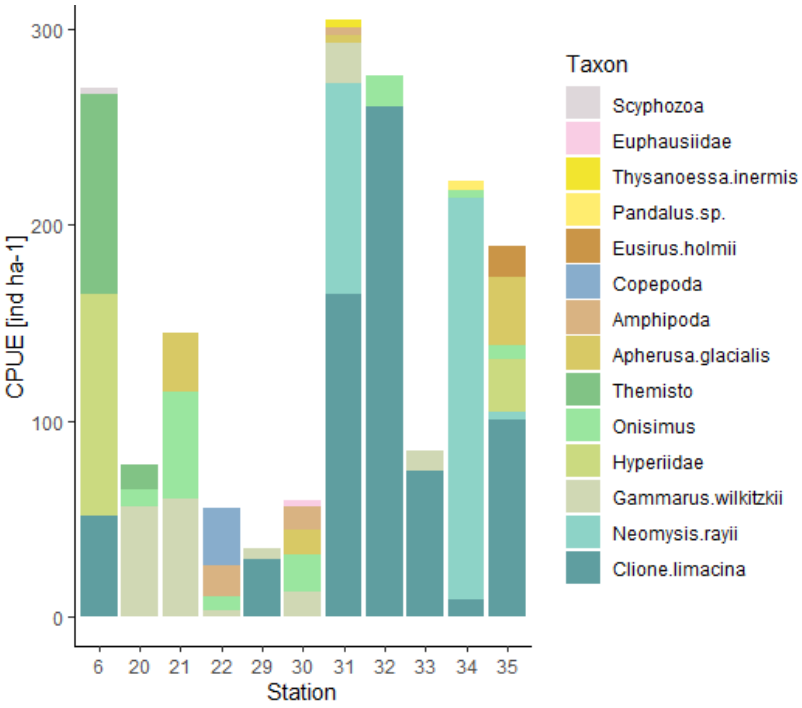

Figure 7: Catch-per-unit-effort of macrozooplankton (individuals per hectare) captured in a Surface and Under-Ice Trawl along the Chukchi and Beaufort shelves during November 2019. Although standardized for effort (area swept by trawl), the net often filled up with ice so density estimates are not reliable. All stations were sampled within the ice except station 6. However, relative species composition is assumed to be comparable across stations.

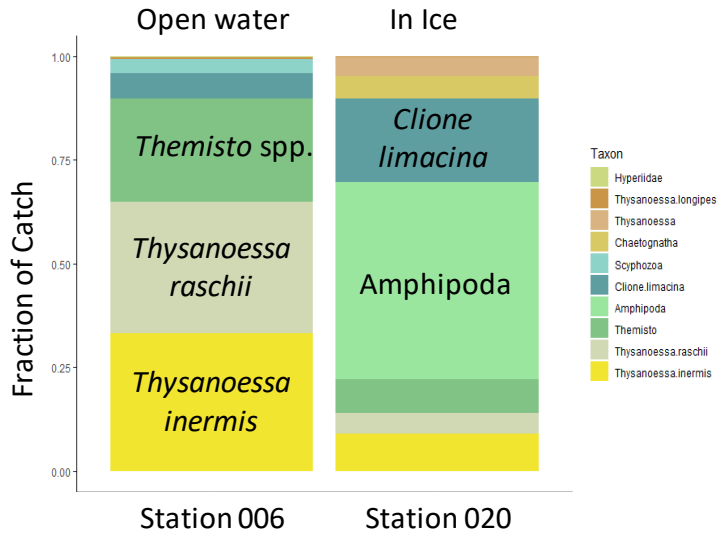

Figure 8: Relative composition of the midwater macrozooplankton community(0–200 m) sampled by a Methot trawl at one open-water station (006) in the western Beaufort Sea and one ice-covered station in the eastern Beaufort Sea.

Arctic Cod

Under-ice abundances

We captured Arctic cod in each SUIT haul, ranging from 1 fish at the open-water fishing station 006 near the ice edge to 37 fish at station 030, located just off the mouth of Barrow Canyon along the slope (1,550 m, see Figure 2). A total of 149 Arctic cod were captured under the ice in SUIT hauls (Figure 9, Table A1 in Appendix 2) and 18 Arctic cod were captured in the water column (0–200 m) at the open water station. The density of Arctic cod under the ice ranged from 227 per km^2 to 12,359 per km^2 (Table 2). A second Methot trawl in the ice (station 020) did not catch any fish. Three polar cod (*Arctogadus glacialis*) were captured in the SUIT at the easternmost station and one polar cod was captured in the midwater at the open-water station. All *A. glacialis* were initially identified as *B. saida* in the field and were only later re-classified as *A. glacialis* based on metabarcoding at the Catholic University of Leuven. No other species were caught under the sea ice, but two Arctic sandlance (*Ammodytes hexapterus*) and five threespine stickleback (*Gasterosteus aculeatus*) were caught at the only open-water fishing station (006). The capture of these stickleback, which typically prefer fresh and brackish water, at a station almost 50 miles offshore at the shelfbreak was unexpected. However, threespine stickleback have been reported up to 800 km offshore (Mecklenburg *et al.*, 2002).

Table 2: Summary of Arctic cod catches and catch-per-unit-effort at 11 stations sampled with Surface and Under-Ice Trawl (SUIT) during November 2019.

Station	*Date*	*Longitude*	*Latitude*	*Depth (m)*	*Ice thickness (cm)*	*Arctic cod (#)*	*Area swept (m^2)*	*CPUE (# km^{-2})*
006	11/11/2019	-151.92	71.58	760	0	1	4401	227
020	11/14/2019	-146.37	70.92	169	44.4	6	2908	2,063
021	11/15/2019	-147.93	71.35	2382	39.9	31	2508	12,359
022	11/16/2019	-148.50	71.24	1286	31.7	7	3841	1,823
029	11/18/2019	-151.04	71.32	200	15.9	2	2163	924
030	11/18/2019	-153.39	71.98	1550	26.9	37	3993	9,267
031	11/19/2019	-154.07	72.19	1894	22.0	17	3117	5,454
032	11/19/2019	-155.72	72.61	2550	23.0	6	1630	3,682
033	11/19/2019	-156.53	72.58	1553	12.6	2	1182	1,692
034	11/20/2019	-156.71	72.83	2059	57.1	21	2810	7,473
035	11/20/2019	-157.47	72.79	986	45.7	19	3243	5,858
Mean				1399	29.0	13.5	2891	4620

Arctic cod (*B. saida*) ranged in length from 51 to 112 mm TL with one larger specimen at 142 mm (Figure 10). In contrast, all four *A. glacialis* were smaller than any of the *B. saida* at 43–47 mm. Weights, as measured on board, ranged from 0.90 to 7.35 g except for the single large specimen at 17.25 g. Mean weights per station varied substantially at the Beaufort Sea stations but were more consistent in the Chukchi Sea (Figure 11). Mean weight at station 021 was strongly influenced by the single large specimen and decreased from 3.39 to 2.93 g when this outlier was excluded. However, the station still had the largest average mean weight after excluding the large specimen. Individual weights increased approximately as a cubic function of length, as would be expected (Figure 12).

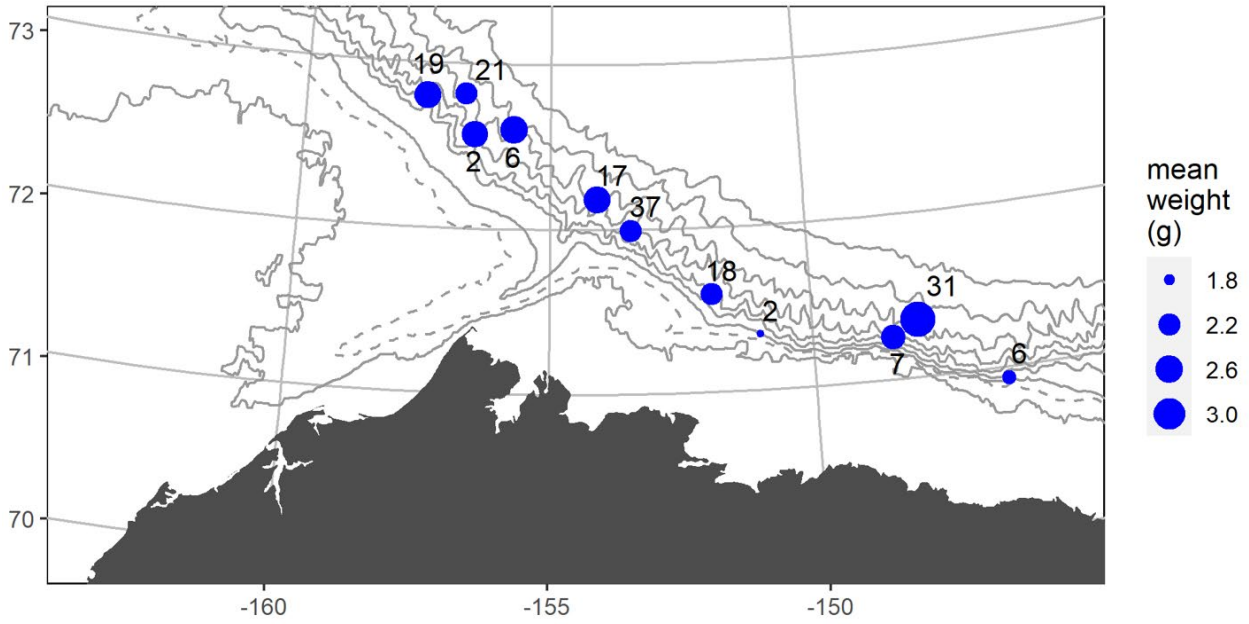

Figure 9: Catch-per-unit-effort (CPUE in numbers per average volume filtered) of Arctic cod (*Boreogradus saida*) at 11 SUIT fishing locations occupied during the Go-West cruise in November 2019.

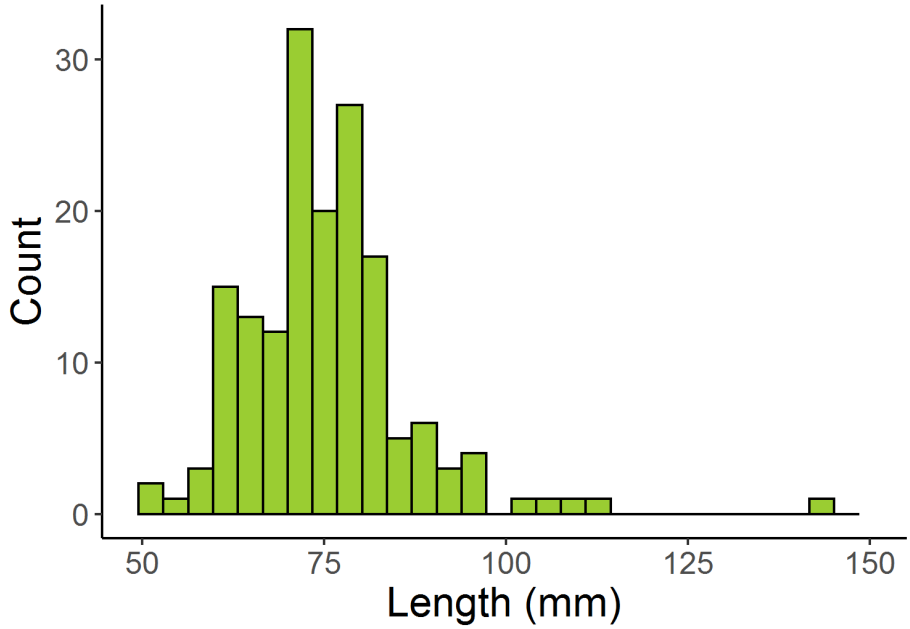

Figure 10: Distribution of the total length (TL) of 166 Arctic cod (*Boreogadus saida*) captured along the Chukchi and Beaufort slopes in November 2019.

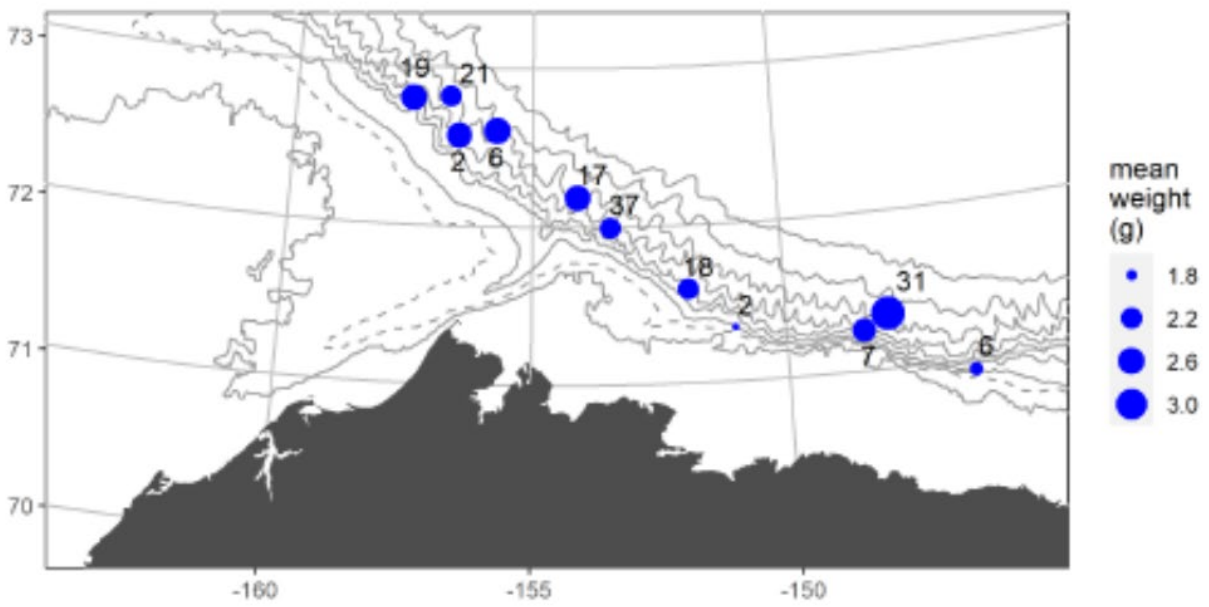

Figure Figure 11: Mean weight (g) and number of Arctic cod (*Boreogradus saida*) captured at 11 SUIT fishing locations occupied during the Go-West cruise in November 2019.

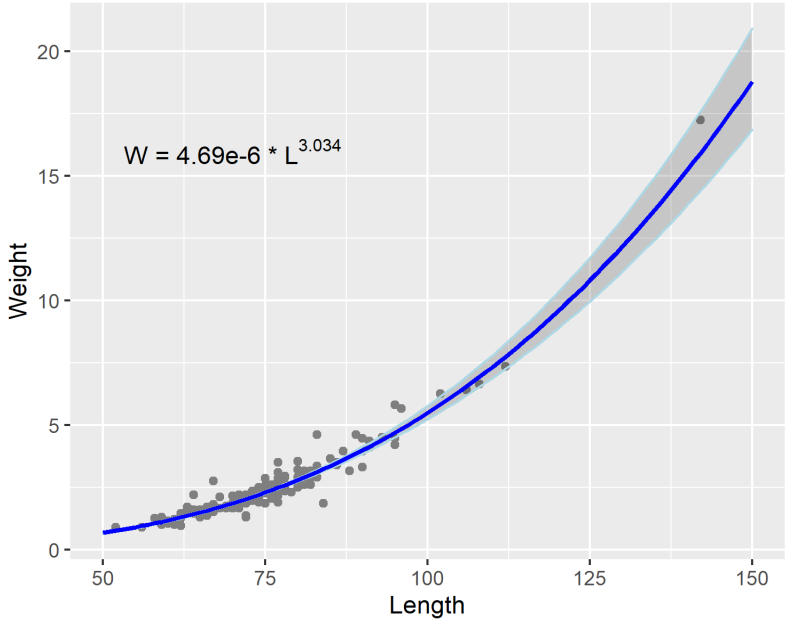

Figure 12: Weight (g) at length (mm) of 163 Arctic cod captured in November 2019.

Catch per unit effort of Arctic cod showed some spatial variability across the study region with lower catches at some of the shallower stations along the outer shelf of the Beaufort Sea and higher catches at deeper stations with heavier sea ice. Regression analyses confirmed a significant relationship between the number of Arctic cod captured, after adjusting for differences in effort, and bottom depth (neg. binomial regression: $R^2 = 0.38$, $p = 0.006$) or ice thickness (neg. binomial regression: $R^2 = 0.32$, $p = 0.006$), suggesting an increased association between Arctic cod and sea ice as the ice grows (Figure 13).

Exploratory correlation analyses did not show significant relationships with temperature, salinity, nutrient concentrations, chlorophyll concentrations, or the abundances of individual macrozooplankton species, with one exception. We found a strong positive relationship between the CPUE of Arctic cod and the CPUE of *Onisimus* spp. ($r = 0.78$; $p = 0.005$), which is a potential prey species for larger Arctic cod, but may also compete with Arctic cod for similar prey.

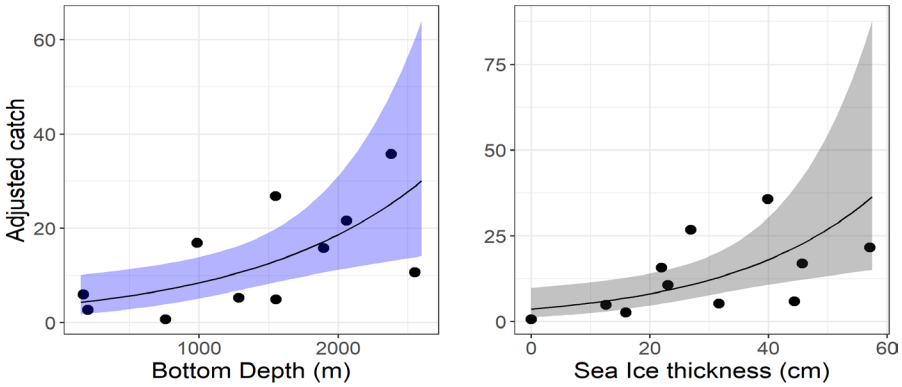

Figure 13: Catch rates for Arctic cod (number of fish per average volume filtered) captured along the Chukchi and Beaufort slopes as a function of bottom depth (left) and sea-ice thickness (right) with predicted values and 95% confidence bands from separate negative binomial regressions of counts with effort as an offset.

Arctic cod population structure

Samples from the Chukchi and Beaufort Sea shelf and slope regions collected under the ice during November 2019 contributed to an Arctic-wide study of the population structure and connectivity of Arctic cod (Maes, 2022). The study used 812 high-quality single nucleotide polymorphisms (SNPs) sequenced from genotyping-by-sequencing to assess the circumpolar population structure as well as local and large-scale connectivity patterns. An AMOVA revealed overall low but significant levels of genetic divergence among Arctic cod samples ($F_{ST} = 0.033$, $p = 0.001$). Low differentiation was also apparent in pairwise F_{ST}-values ranging from zero to 0.108 (between Chukchi Sea and W-Greenland). A STRUCTURE analysis indicated that $K = 3$ or $K = 4$ is the most likely true number of clusters (Figure 14). At a circumpolar scale, three clear, large-scale groups were genetically differentiated: Alaskan Arctic (Beaufort and Chukchi Sea), Transpolar Drift (Iceland, Laptev Sea, Northeast Canada), and Europe (Central Arctic Ocean, Svalbard, Northeast Greenland, and West Greenland) with sub-structuring detected in all these groups. A fourth genetically differentiated group included at least two individuals from Northeast Greenland and the Laptev Sea. Finer-scale structure within the three main groups was evident in the DAPC results (Figure 15), which differentiated Northeast Canada from other regions and encompassed a gradient from Northeast Greenland and Svalbard across the Central Arctic Ocean, Iceland, the Laptev Sea and West Greenland to the Alaskan Arctic.

The Alaskan Arctic group was genetically homogenous ($F_{ST} = 0$, $p = 0.609$) on the circumpolar scale, in agreement with previous analyses (Nelson *et al.*, 2020). However, individuals from the Chukchi Sea and the Beaufort Sea clearly separated along the first principal component in a PCA with minimal overlap (Figure 16). Arctic cod in the Alaskan Arctic group are genetically differentiated from those in other locations around the Arctic but were least differentiated ($FST < 0.024$) from Arctic cod in the Iceland, Laptev Sea, and Northeast Canada samples (Figure 16). This is consistent with the STRUCTURE results, which show that the Alaskan Arctic shares genotypes with Iceland, the Laptev Sea, and NE Canada.

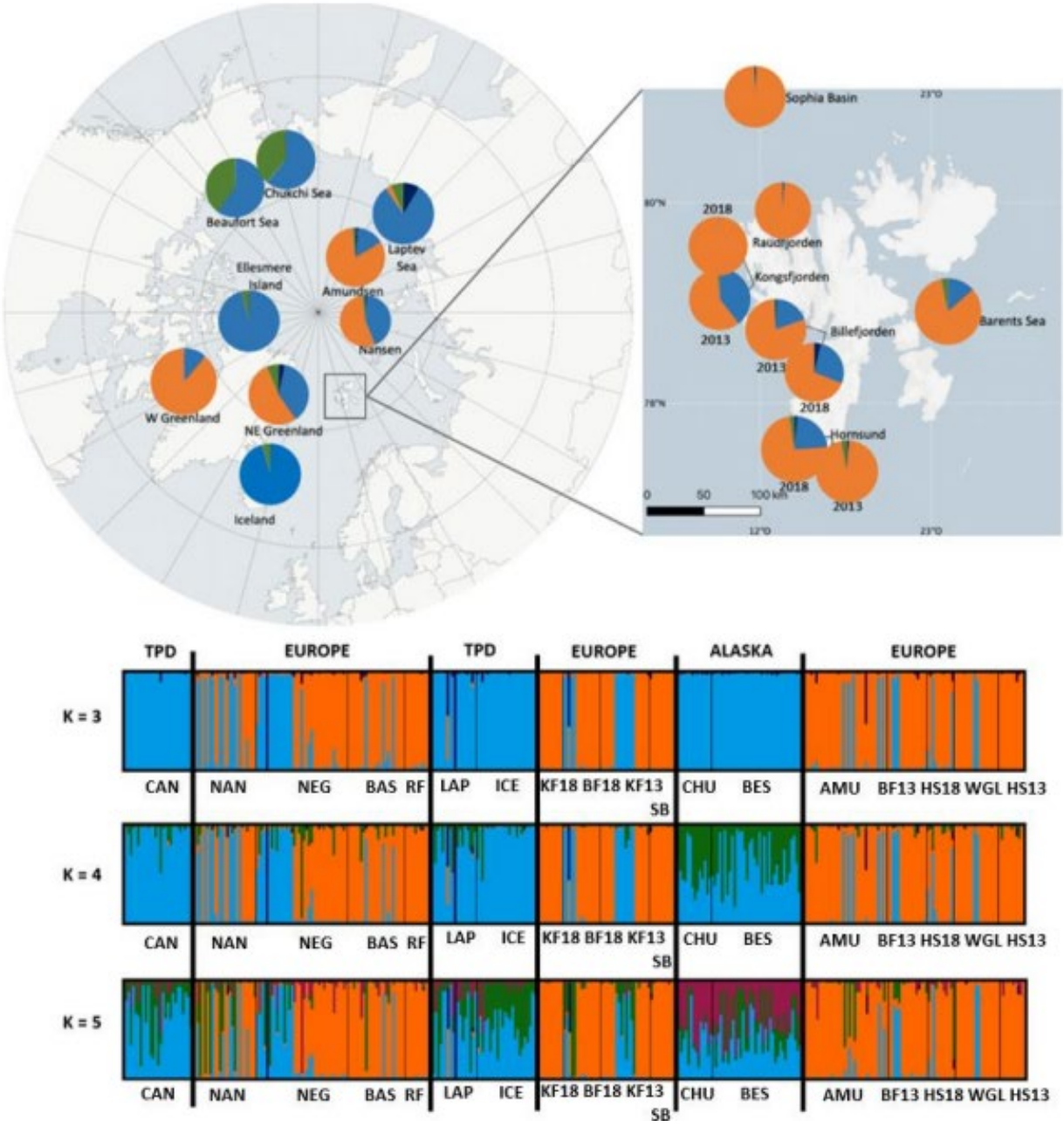

Figure 14: Population structure of Arctic cod derived from STRUCTURE analysis of 362 individuals using 812 SNPs. The geographic plot shows results from k=4 groups and the bar plot shows results for K = 3, K = 4, and K = 5. The colors of the pie chart represent the likelihood of membership to each of the four clusters identified by STRUCTURE. Each vertical colored line in the bar plot represents an individual and the proportion of the color corresponds to the probability that the individual is a member of a specific cluster. Dark vertical lines delineate the study regions. Based on the dominating genotype (color), the three large-scale clusters are composed of: (1) Svalbard, NE Greenland, W Greenland, and Amundsen and Nansen Basin in orange; (2) Beaufort and Chukchi Sea in green; (3) Iceland, Ellesmere Island (i.e., NE Canada) and Laptev Sea in blue. At least one individual collected in the Laptev Sea and at least one individual from NE-Greenland (dark blue) form a fourth group. From Maes (2022).

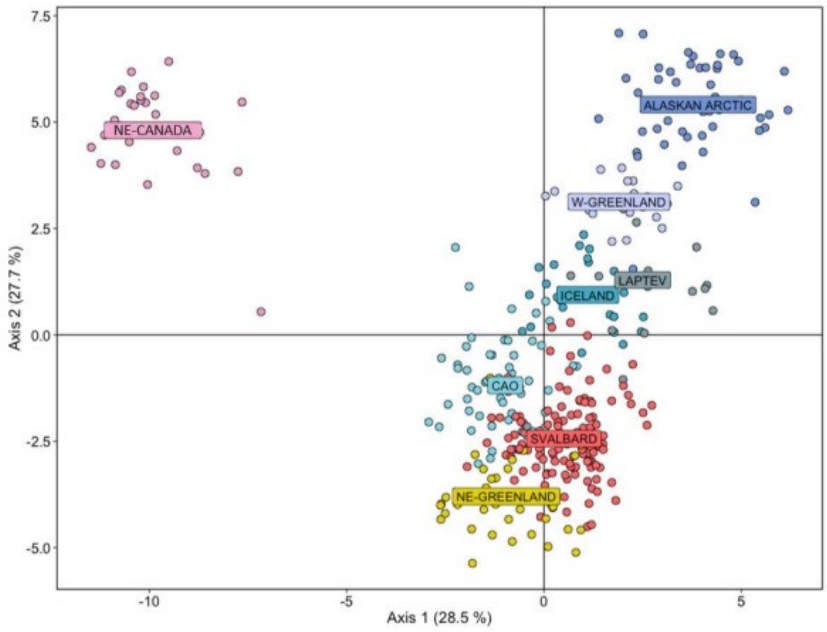

Figure 15: Population genetic structure based on Discriminant Analysis of Principal Component (DAPC) of putative Arctic cod groups on a circumpolar scale after retaining the first 50 PCs. From Maes (2022).

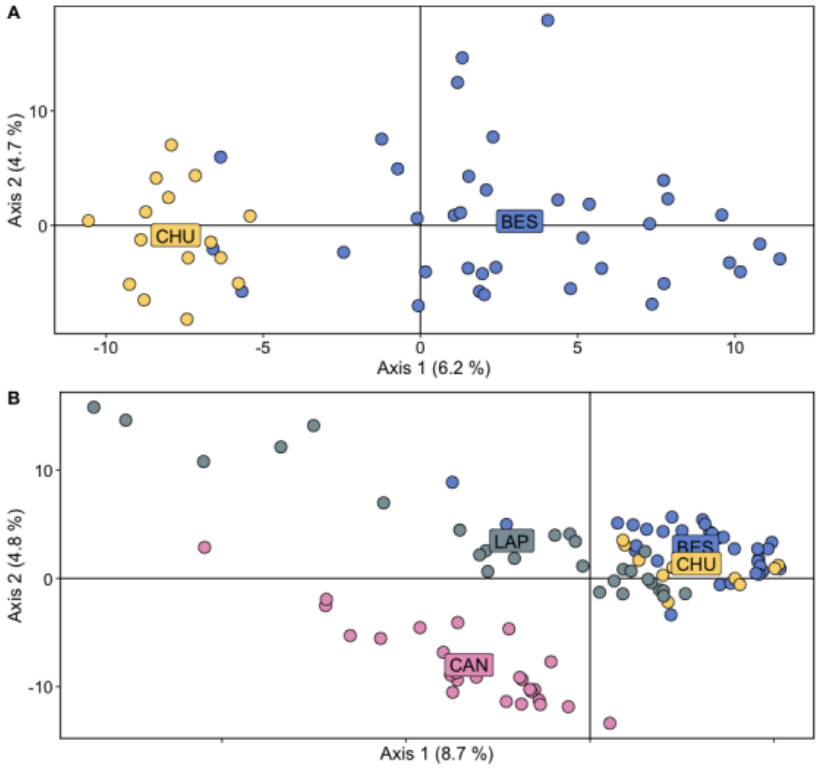

Figure 16: Principal Component Analysis (PCA) of Arctic cod sampled in (A) the Beaufort (BES) and Chukchi seas (CHU), and (B) the Beaufort, Chukchi, and Laptev (LAP) seas and NE Canada (CAN). From Maes (2022).

Arctic cod diets

In total, 36 out of 107 stomachs (33.6 %) were empty based on visual inspection during sampling. A total of 85 Arctic cod stomachs were used for DNA metabarcoding of stomach contents, while stomach contents of the remaining 22 stomachs were visually examined. Twenty-nine samples were removed after metabarcoding due to the low number of total reads (< 20 reads), including 20 stomachs that were considered empty based on visual analysis. The final diet data set contained 308,079 reads (where the number of reads for a given diet item provides a rough measure of abundance) and 362 amplicon sequence variants (ASVs, corresponding to species or taxa) from 56 Arctic cod stomachs. Most taxonomic assignments (44 of 49) were at the species level, except for five taxa that could only be identified with certainty at the genus level. A DNA barcode belonging to the decapod *Hyas* sp. matched both *H. coarctatus* and *H. lyratus*, hence species-level identification was not conclusive. However, extensive plankton sampling in the Chukchi Sea in 2012, 2013, and 2017 identified large numbers of *H. coarctatus* but no *H. lyratus*, which typically occur farther south (Jared Weems, Kodiak, AK, unpublished data). Thus, we assume that all *Hyatus* sp. are *H. coarctatus*. Likewise, while some *Acartia* sp. barcodes unambiguously matched *A. longiremis*, for others the species-level identification was unclear (*A. longiremis* or *A. hudsonica*). One *Anisakis* sp. barcode matched *A. simplex* and *A. typical*, which could not be resolved based on the similarity of sequences or tree-based identification in BOLD. The molecular identification of jellyfish from the family Semaeostomeae was particularly challenging. Most barcodes belonging to the genus *Cyanea* could not be assigned to a species with certainty. Tree-based identification in BOLD suggests that *Cyanea* barcodes probably belong to *C. tzetlinii* or *C. capillata*; however, this is not conclusive. Furthermore, one *Aurelia* sp. barcode could not be assigned to the species level but matched with 99.7% with an unidentified *Aurelia* sp. barcode from Russia.

The diet of Arctic cod in our sample consisted of at least 48 different species belonging to eight phyla. Arctic cod fed on a broad spectrum of prey items with calanoid copepods as dominating order in terms of both relative read abundance and frequency of occurrence (82.1% of stomachs), followed by pelagic ostracods (46.4%) and sea ice-associated amphipods (28.6%). The most common prey species was the pelagic ostracod *Boroecia maxima* (46.4% of stomachs), followed by the calanoid copepods *Calanus hyperboreus* (44.6%) and *Metridia longa* (42.9%) (Figure 17). These prey species were consumed by Arctic cod juveniles of all sizes. Arctic cod that consumed fish (presumably eggs and/or larval stages) ranged in length from 76 to 108 mm TL. Furthermore, the mysid shrimp *Neomysis rayii* was only consumed by larger Arctic cod ranging from size 76 to 82 mm TL.

Based on alpha diversity measures, there was no difference between the diversity of the diet in Arctic cod from the Chukchi and Beaufort seas, nor between size classes or stations with varying sea-ice coverage. The observed diversity (i.e., number of ASVs) was higher, but not significantly different, for Arctic cod sampled on the continental slope and in deep water stations compared to the continental shelf. Although the frequency of occurrence of prey items varied between geographical areas (slope region, deep water, and shelf region), the ostracod *B. maxima* and calanoid copepods *C. hyperbore*us, *P. glacialis,* and *M. longa* were, in general, the most common prey items in all areas.

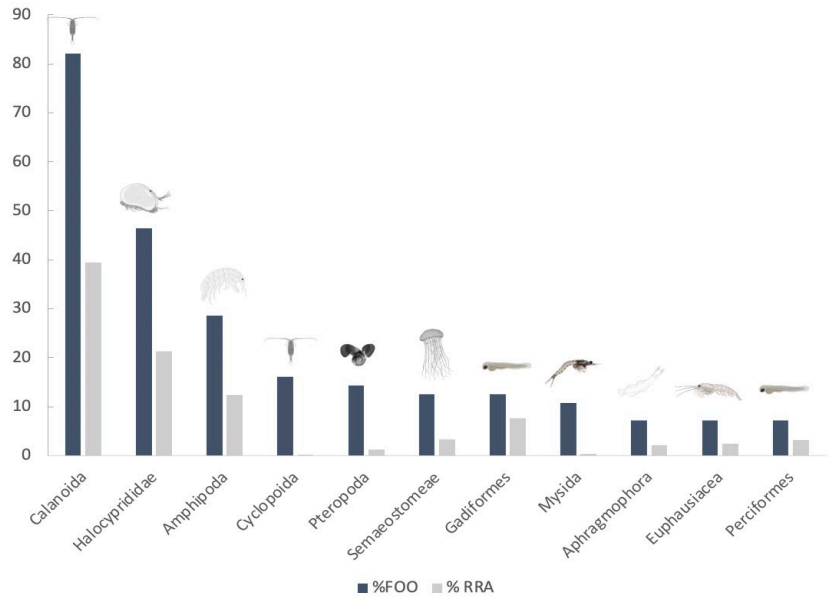

Figure 17: Frequency of occurrence (% FOO; dark blue) and relative read abundance (% RRA; light grey) of most common prey orders detected by DNA metabarcoding in polar cod (Boreogadus saida) stomachs in the Alaskan Arctic. Based on Maes (2022).

Table 3: Overview of prey taxa found in >10 % of the Arctic cod stomachs sampled as identified by DNA metabarcoding. Frequency of occurrence (% FOO) and relative read abundance (% RRA) are given per sampling region (BES, CHU) and for all individuals combined (ALL).

Order	Species	% FOO BES	% FOO CHU	% FOO ALL	% RRA BES	% RRA CHU	% RRA ALL
Calanoida	*Acartia* sp.	5.4	10	7.1	0.2	1.2	0.4
Calanoida	*Gaetanus tenuispinus*	0	20	3.6	0	0.4	0.01
Calanoida	*Calanus glacialis*	12.5	0	12.5	4.4	0	3.4
Calanoida	*Calanus hyperboreus*	39.3	30	44.6	16.8	10.1	15.5
Calanoida	*Pseudocalanus acuspes*	12.5	10	14.3	0.4	0.4	0.4
Calanoida	*Pseudocalanus minutes*	8.9	10	10.7	0.8	0.2	0.7
Calanoida	*Pseudocalanus newmani*	5.4	10	7.1	<0.1	0.2	0.1
Calanoida	*Paraeuchaeta glacialis*	28.6	20	32.1	8.1	10.1	8.1
Calanoida	*Heterorhabdus norvegicus*	12.5	0	12.5	<0.1	0	0.2
Calanoida	*Metridia longa*	35.7	40	42.9	7.0	1.8	5.8
Calanoida	*Scolecithricella minor*	3.6	20	7.1	<0.1	0.1	<0.1
Cyclopoida	*Oithona similis*	12.5	20	16.1	<0.1	0.7	0.1
Amphipoda	*Apherusa glacialis*	17.9	0	17.9	9.1	0	7.0
Mysida	*Neomysis rayii*	3.6	40	10.7	<0.1	32.7	7.6
Halocyprida	*Boroecia maxima*	37.5	50	46.4	21.1	18.0	21.3
Gadiformes	*Arctogadus glacialis*	5.4	30	10.7	1.7	11.0	3.3
Semaeostomeae	*Chrysaora melanaster*	8.9	10	10.7	1.0	<0.1	1.1
Pteropoda	*Clione limacina*	1.8	30	7.1	<0.1	12.4	2.2
Pteropoda	*Limacina helicina*	5.4	20	8.9	0.1	0.6	0.2
Diphyllobothriidea	*Diphyllobothrium schistochilos*	1.8	10	3.6	<0.1	0.1	<0.1

Out of 22 Arctic cod stomachs that were visually analyzed, 16 contained prey. Morphological identification, however, was difficult due to high digestion levels (average degree of digestion 3.4) (Table 4). Three taxa were identified to the species level: *Pareuchaeta glacialis* (copepodite stages IV and V, and adult females), *Metridia longa* (copepodite stage V and adult females), and *Calanus hyperboreus* (copepodite stage V). The remaining prey could be classified as copepod and mysid fragments, gammarid amphipods, and *Pseudocalanus* spp. (copepodite stage V).

Table 4: Summary of stomach content of polar cod (*Boreogadus saida*) based on visual identification per station with n = total number of individuals, TL = total length (cm), and RFI = recognizable food items. Both average weight and average stomach content weight are given in grams. Details on morphological measurements are also provided per station. Frequency of occurrence (% FOO) is given for stations 6, 21, 22, and 30, and for the total number of fish.

	6	**21**	**22**	**30**	**Total**
N	1	8	3	10	22
Average TL	75	79	78.3	70.8	75.4
Average weight	2.4	3.4	3.6	2.1	2.7
Digestion degree	4	2.3	3.7	2.5	3.4
RFI	1	33	10	13	56
n empty stomachs	0	3	0	3	6
Stomach content					
Ave. number recognizable food items (N. ind^{-1})					
Calanus hyperboreus	0	0	0	0.1	0.05
Copepod fragments	0	0	0.7	0.3	0.2
Gammarid amphipod	0	0	0.3	0	0.05
Metridia longa	0	3.3	0	0.1	1.2
Mysidae fragments	0	0	0	0.1	0.05
Pareuchaeta glacialis	1	0.9	2.3	0.6	1.0
Pseudocalanus spp.	0	0	0	0.1	0.05
Frequency of occurrence (% FOO)					
Calanus hyperboreus	0	0	0	10.0	4.5
Copepod fragments	0	0	66.7	20.0	18.2
Gammarid amphipod	0	0	33.3	0	4.5
Metridia longa	0	37.5	0	10.0	18.2
Mysidae fragments	0	0	0	10.0	4.5
Pareuchaeta glacialis	100	62.5	33.3	50.0	54.5
Pseudocalanus spp.	0	0	0	10.0	4.5

Arctic cod gut microbiome

This study contributed to the first ecological baseline of bacterial diversity in the gut microbiome of Arctic cod. Like other marine fishes, the Arctic cod gut microbiome was diverse and consisted of the phyla Actinobacteria, Bacteroidota, Deinococcus-Thermus, Firmicutes, and Proteobacteria with little differentiation among ages, seasons, and geographical regions. Samples in the Alaskan Arctic were characterized by the presence of transient microbiota such as the cyanobacteria *Synechococcus* sp. and Verrucomicrobia, reflecting the influence of under-ice habitat on the microbial composition. The gut microbial composition differed significantly between the Barents Sea and the Alaskan Arctic, at least in part reflecting the fact that samples were taken during the summer in the Barents Sea and under the ice

during late fall in the Alaskan Arctic. A high number of unidentified sequences highlight the limited baselines for local bacterial communities.

Arctic cod body condition

A total of 60 Arctic cod were available for measuring whole-body lipid content (liver + muscle tissue). An additional 100 tissue samples were available to estimate lipid density in muscle tissue. Lipid density in muscle tissue was strongly and significantly correlated with lipid density in liver tissue for the 60 fish for which both estimates were available ($r = 0.68$, $p < 0.001$). Whole body lipid density varied across stations, and we combined stations within three regions, the eastern Beaufort Slope (stations 021–029, see Figure 1), the area off Barrow Canyon (stations 030/031), and the Chukchi Slope (032–035). Whole body lipid densities decreased with size (ANCOVA partial effect of size: $F = 2.27$, $p = 0.138$) and were higher in the Beaufort Sea compared to the other regions when adjusted for size differences (Figure 18, ANCOVA partial effect of region: $F = 9.14$, $p < 0.001$). The same pattern held for the expanded data set based on muscle tissue (Figure 19, ANCOVA partial effect of region: $F = 17.47$, $p << 0.001$; partial effect of size: $F = 44.1$, $p << 0.001$).

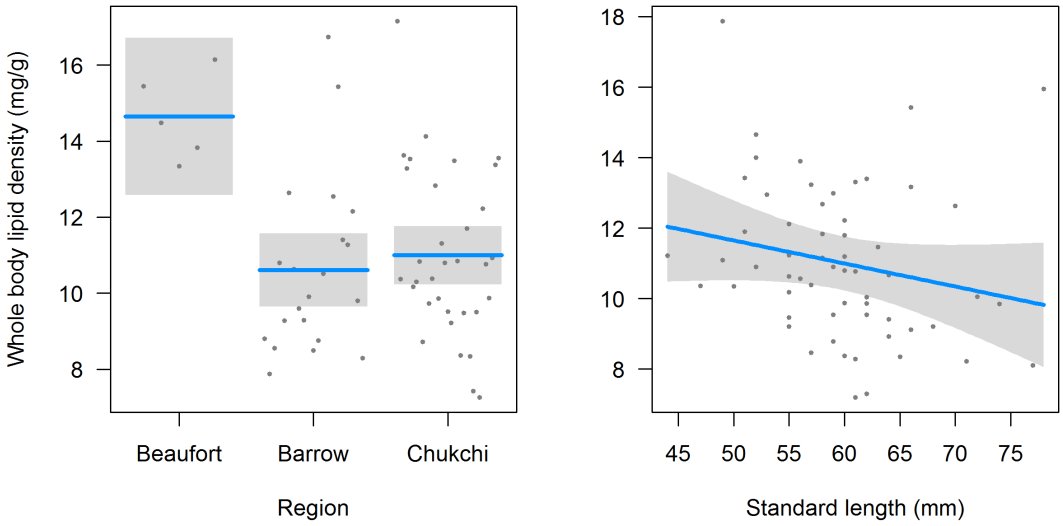

Figure 18: Lipid density of Arctic cod collected at five stations along the eastern Beaufort Slope (021) and the Chukchi Sea slope (030–035). Density is based on total body lipids and whole-body wet weight. Blue lines denote predicted mean lipid density from an analysis of covariance with 95% confidence bands. Regions denote the eastern Beaufort Slope (stations 021–029, see Figure 1), the region off Barrow Canyon (stations 030/031), and the Chukchi Slope (stations 032–035).

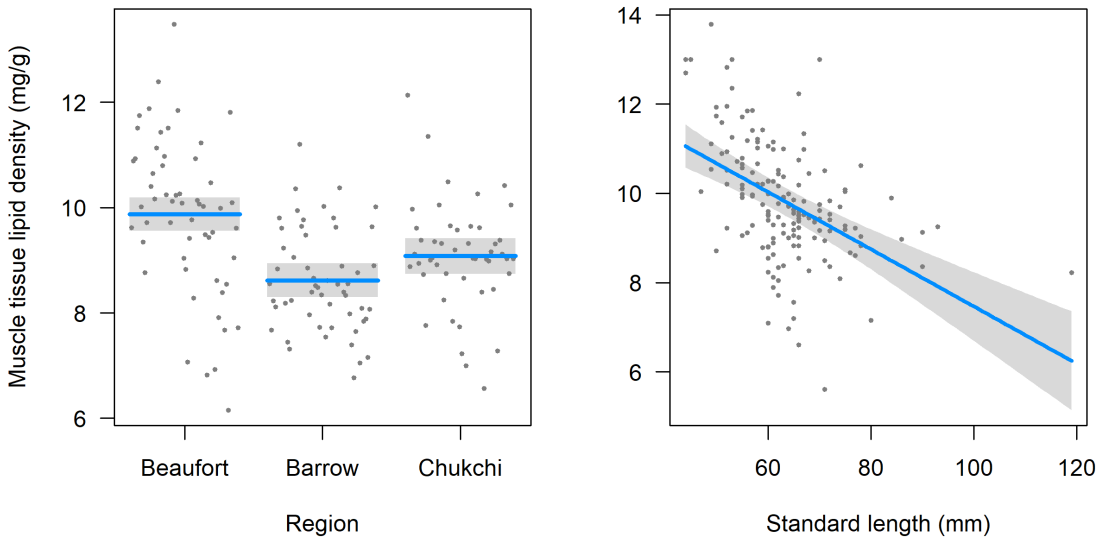

Figure 19: Lipid density of Arctic cod collected in three regions along the Chukchi and Beaufort slopes: eastern Beaufort Slope (stations 021–029), off Barrow Canyon (stations 030/031), and the Chukchi Slope (stations 032–035). Density is based on muscle tissue lipids and muscle wet weight. Blue lines denote predicted mean lipid density from an analysis of covariance with 95% confidence bands.

Arctic cod collected under the sea ice in fall were heavier at a given size than Arctic cod collected during late summer on the Chukchi shelf (Figure 20). However, this was largely due to high water content, while the total lipid content and the estimated total fatty acid content per fish were considerably lower at a given size for fish collected under sea ice. This suggests a poor energetic condition of the ice-associated juveniles in late fall 2019, compared to juveniles of the same cohort sampled earlier in the year.

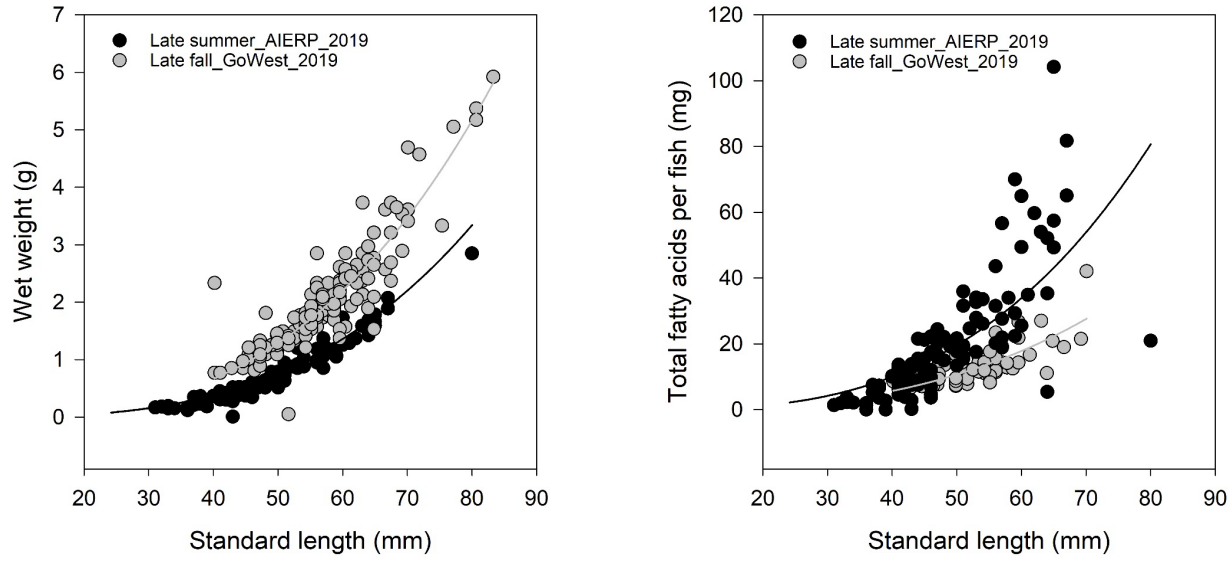

Figure 20: Wet weight (left) and total fatty acid content per fish (right) at a given size for Arctic cod collected under the sea ice in November 2019 (Go-West, in gray) and during the summer Arctic Integrated Ecosystem Research Program in summer 2019 (black).

To provide context for the lipid reserves of juvenile Arctic cod captured under the ice in late fall, we compared their lipid density (total lipids per unit wet weight) to those from starvation trials at four different temperatures (Copeman *et al.*, 2022a). Laboratory fish at an ambient temperature of -1°C survived approximately twice as long (150 days) as fish kept at 5°C (Figure 21). Regardless of temperature, mortalities of fish consistently occurred when lipid density had decreased to approximately 12.5 mg/g wet weight. Arctic cod sampled under the ice in February had mean (whole-body) lipid densities below the mortality threshold (< 12.5 mg/g) at four stations and a slightly higher lipid density at one station in the Beaufort Sea (station 021) (Figures 18, 21), suggesting that field-caught Arctic cod were close to starvation and would not survive the winter without additional food.

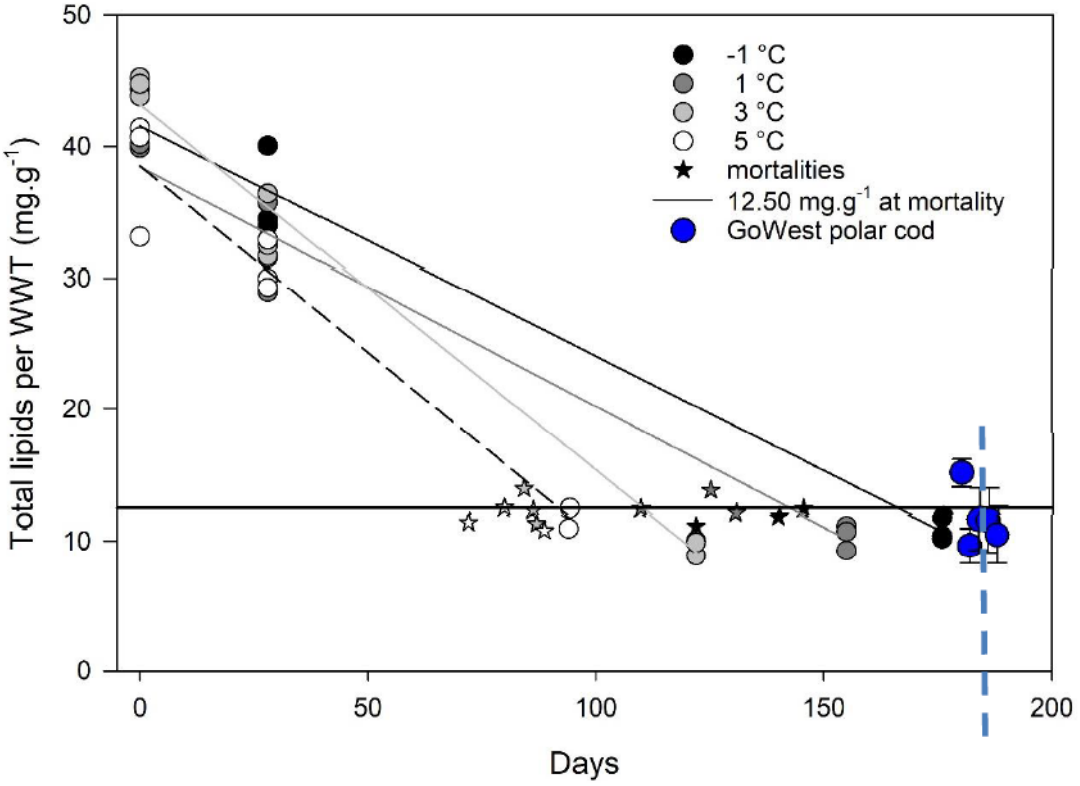

Figure 21: Lipid density (total lipids per unit wet weight in mg/g) of juvenile Arctic cod during starvation trials in the laboratory at four different temperatures (grey dots and fitted lines). Lipid density was measured for a random subset of individuals at the start, on day 30, when mortalities occurred (stars), and when the experiment concluded. The horizontal line denotes the mean lipid density (12.5 mg/g) at which mortalities occurred. Blue dots and bars denote the mean and standard deviation of field-based measurements of lipid density at five stations, plotted arbitrarily along the x-axis for comparison with total lipid content of starving fish. Modified from Copeman et al. (2022a)

Water column abundances and distribution of Arctic cod

The EK80 echosounder detected three Sound Scattering Layers (SSL) between 10 and 25 m, between 25 and 65 m, and 65 and 275 m, respectively (Figure 22). The backscatter was low below 300 m (Figure 23). The average backscatter of the first layer was too shallow to be measured at 18 kHz but was stronger at 200 kHz and lower at 38 kHz (Figure 24a). The frequency-response curve likely indicates the dominance of zooplankton such as chaetognaths or copepods in the top 25 m (Darnis *et al.*, 2017). The presence of both groups and other zooplankton was confirmed by CalVET samples (see 'Zooplankton' section). The

backscatter of the 25–65 m and 65–275 m layers was stronger at the lower frequencies (18, 38, and 70 kHz) than at 120 and 200 kHz, indicating a dominance of swim-bladdered fish (Figure 24b,c). Given the strong dominance of Arctic cod in the pelagic fish community of the Beaufort Sea (>95%; Benoit *et al.*, 2008; Geoffroy *et al.*, 2016) and their presence under the sea ice at each sampling station, we can assume that they dominated the assemblage of the two deeper layers.

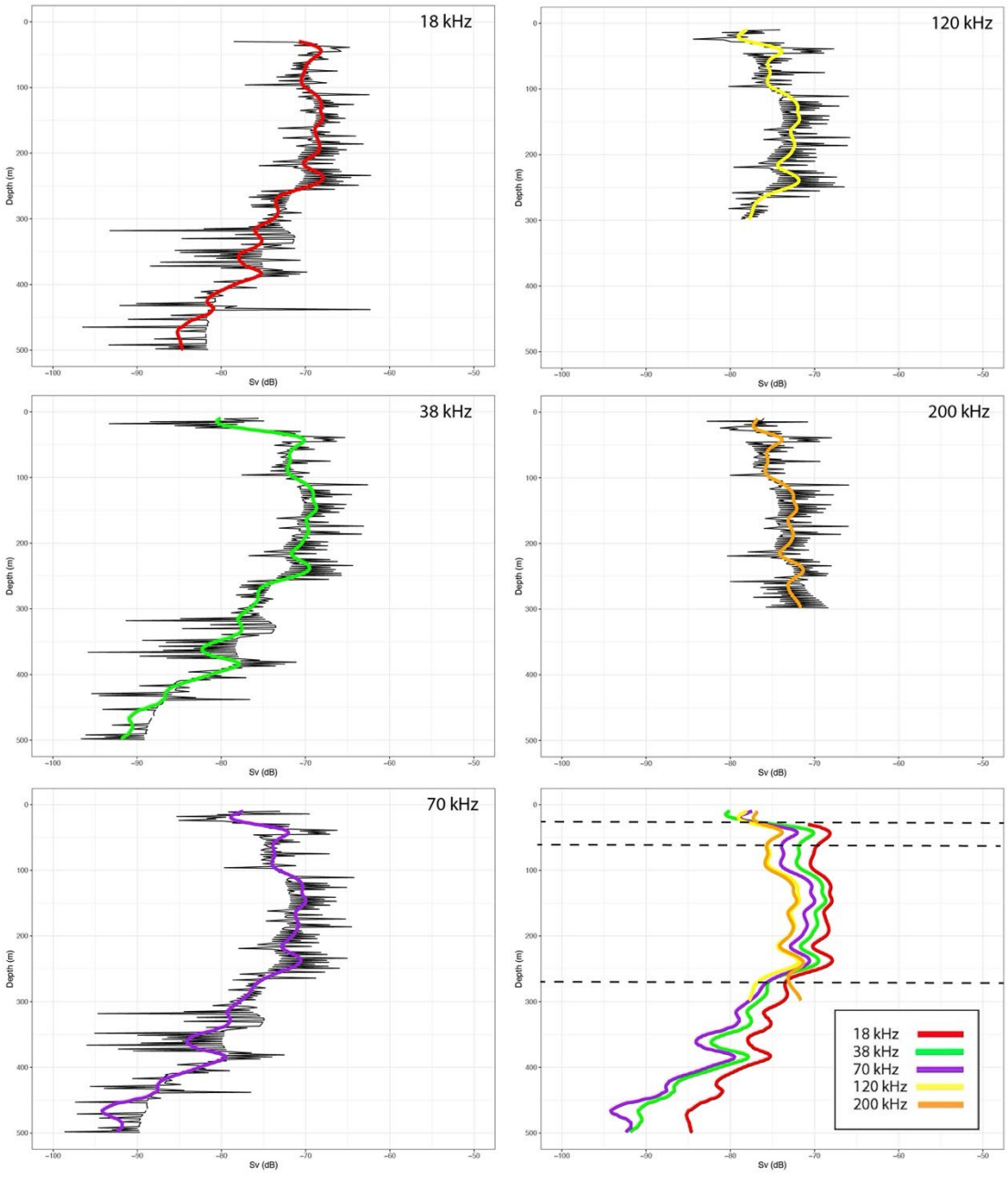

Figure 22: S_v profiles averaged over the duration of the survey at 18, 38, 70, 120, and 200 kHz. The black lines indicate the exported S_v values and the color lines are the Gaussian kernel smoothing with a 25 m vertical resolution. The bottom right panel presents all superposed kernel smoothing curves, and the dashed lines indicate the three vertical layers.

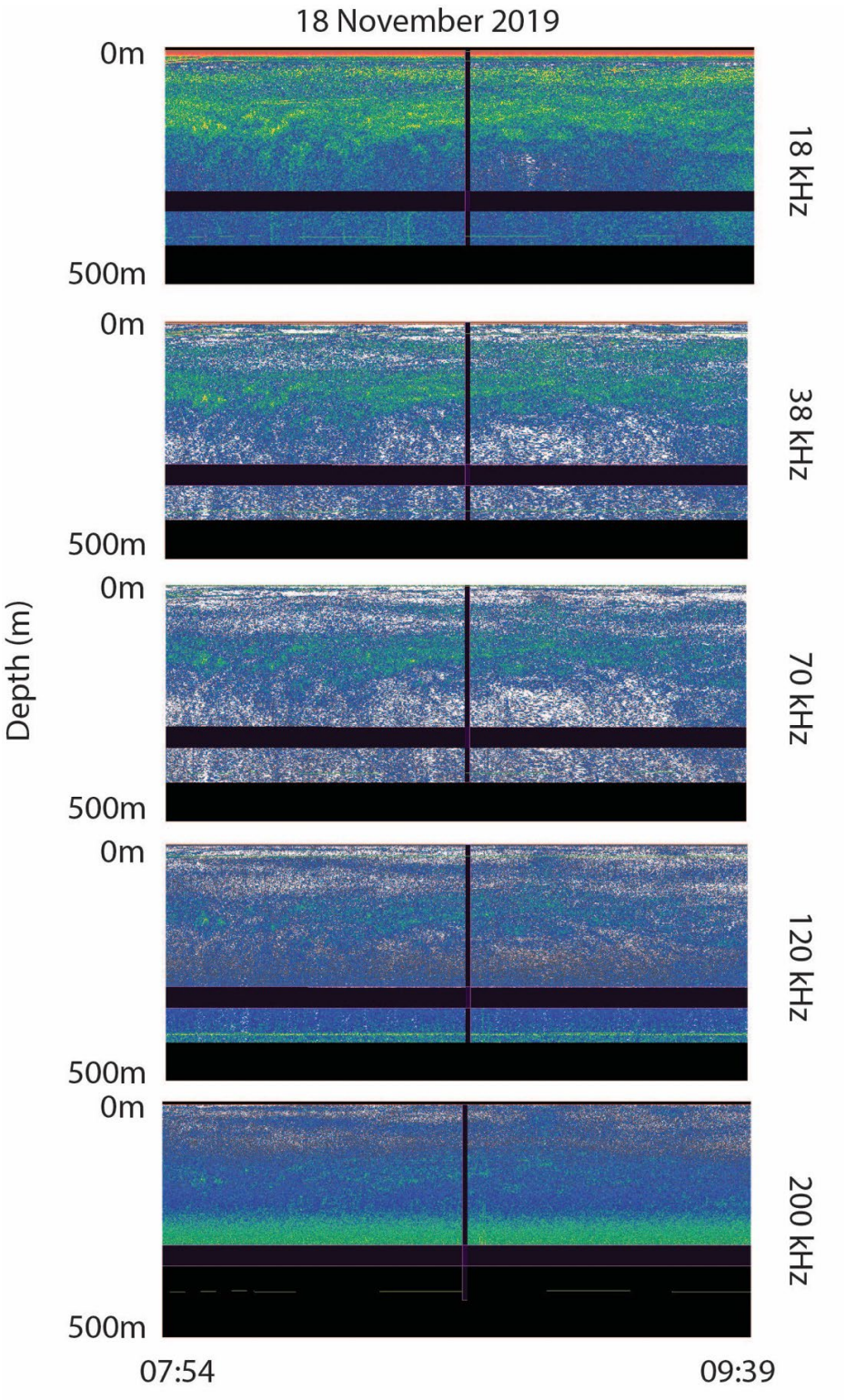

Figure 23: S_v echograms on 18 November. Black areas indicate no data. The color scale varies from -90 to -40 dB. The higher backscatter below 300 m at 120 and 200 kHz was caused by background noise and was not included in the analyses.

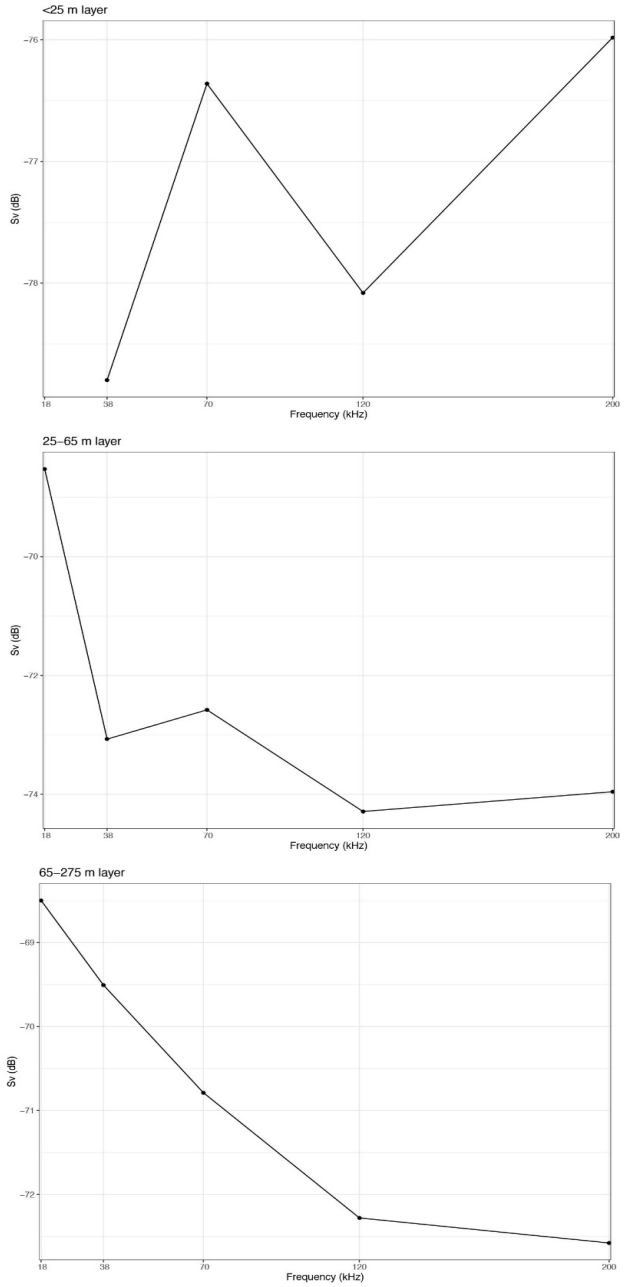

Figure 24: Average frequency response curves of S_v between 10–25 m, 25–65 m, and 65–275 m.

The first (10–25 m) and second (25–65 m) layers were vertically patchy (Figure 25) and formed thin layers (Figure 26). The 65–275 m aggregation was more uniform (i.e. less patchy, Figure 25c) and consistent (Figure 26). Overall, the patchiness was higher over the Chukchi shelf than the slope and the Beaufort Sea (Figure 25d). This might be related to the higher backscatter of zooplankton in the 10–25 m layer over the Chukchi shelf compared to the slope (Figure 27a). In contrast, the backscatter of fish in the 25–65 m and 65–275 m layers was concentrated over the slope (Figure 27b,c), which resulted in an overall higher abundance of organisms over the slope than the shelf (Figure 27d). Denser aggregations of fish were also observed at the shelf break (Figure 28).

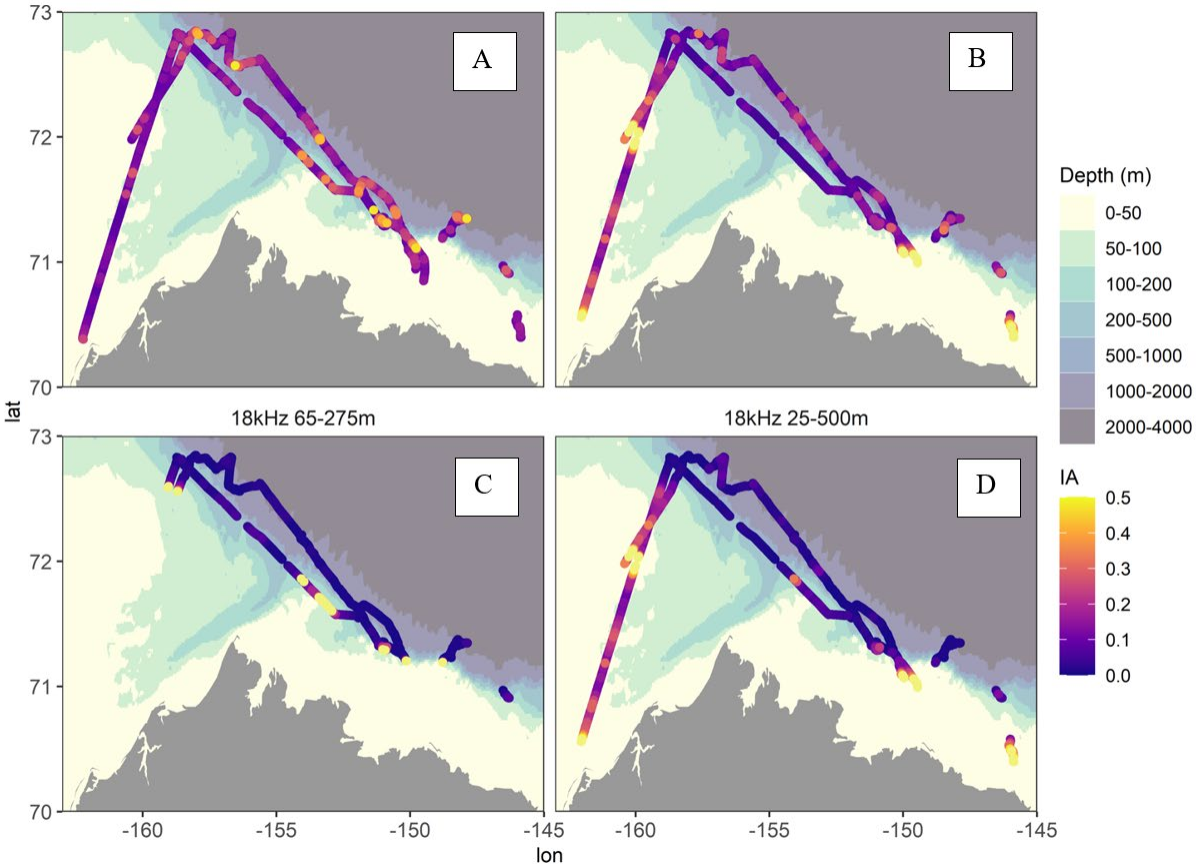

Figure 25: Vertical index of aggregation (IA) along the survey for (A) the 10–25 m layer at 200 kHz; (B) the 25–65 m layer at 18 kHz; (C) the 65–275 m layer at 18 kHz; and (D) the 25–500 m layer at 18 kHz. A higher IA value indicates higher patchiness, and a lower IA value indicates a more uniform distribution. Spatial resolution is 0.25 nm.

We found some evidence of diel vertical migrations (DVM) in acoustic backscatter data. The occurrence of DVM is difficult to assess because the vessel consistently moved between different areas. Clear DVM patterns were observed on November 19–20, when the boat remained in areas >500 m. During this period, part of the deeper SSL moved towards the surface around solar midnight, dividing the deeper SSL into two layers and increasing the dispersion of backscatter (Figure 29). Over these two days, the average center of mass between 25 and 500 m at 18 kHz was 30 m lower around solar noon (21:00–24:00 UTC) than at solar midnight (09:00–11:00 UTC) (130.4 m *vs* 99.7 m, Figure 30). A Target Strength (TS) analysis demonstrated that the targets moving from the deep SSL were weaker and smaller (mean TS = -54.17 dB), while larger individuals (mean TS = -49.91 dB) remained below 200 m (Figure 31). Assuming that these targets were Arctic cod and using the TS-to-length relationship by Geoffroy et al. (2016), vertically migrating fish would have been 5.8 cm long on average and those remaining at mesopelagic depth would have been 11.5 cm.

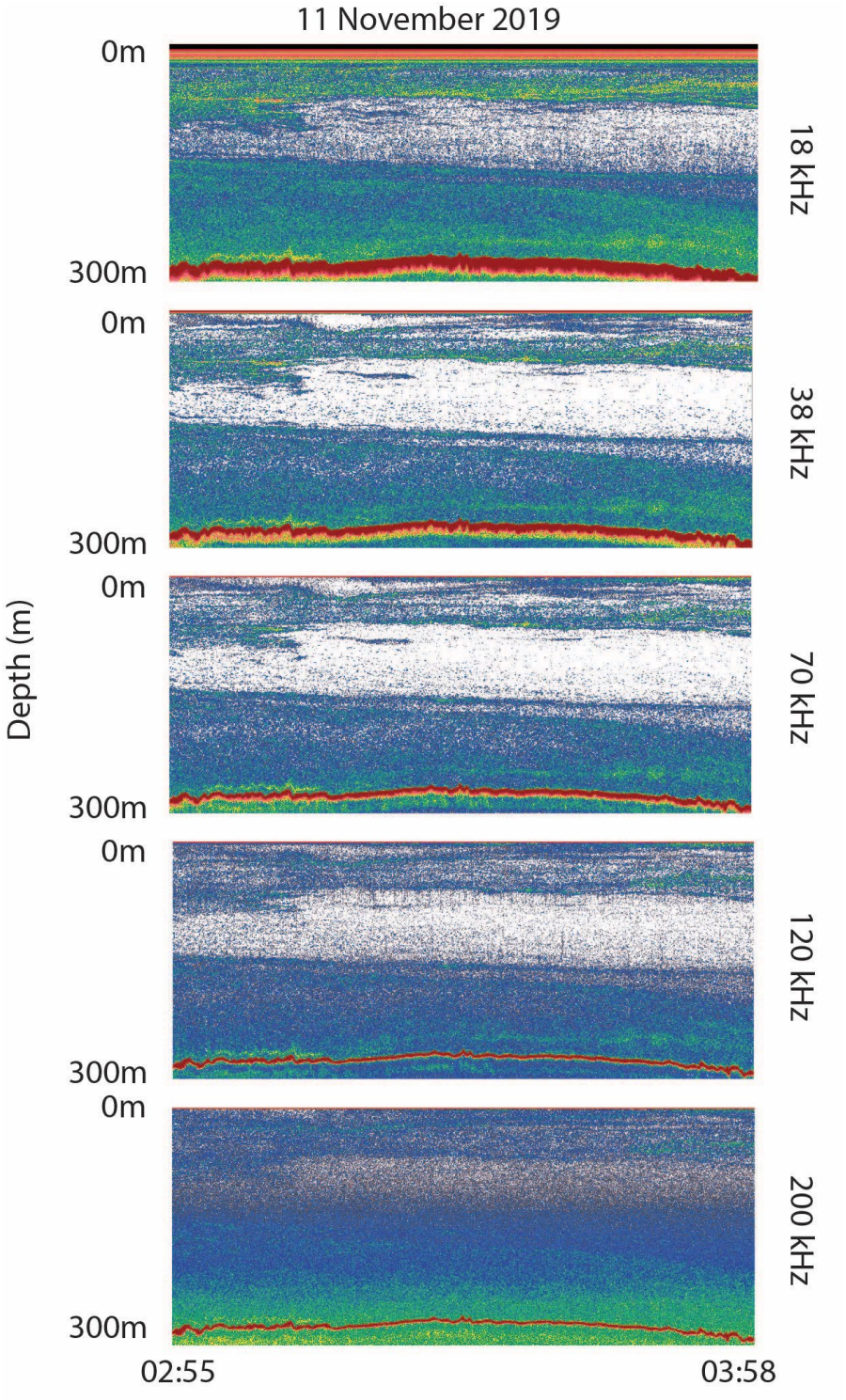

Figure 26: Example of S_v echograms on November 11 showing the different layers at all frequencies. The color scale varies between -90 and -40 dB.

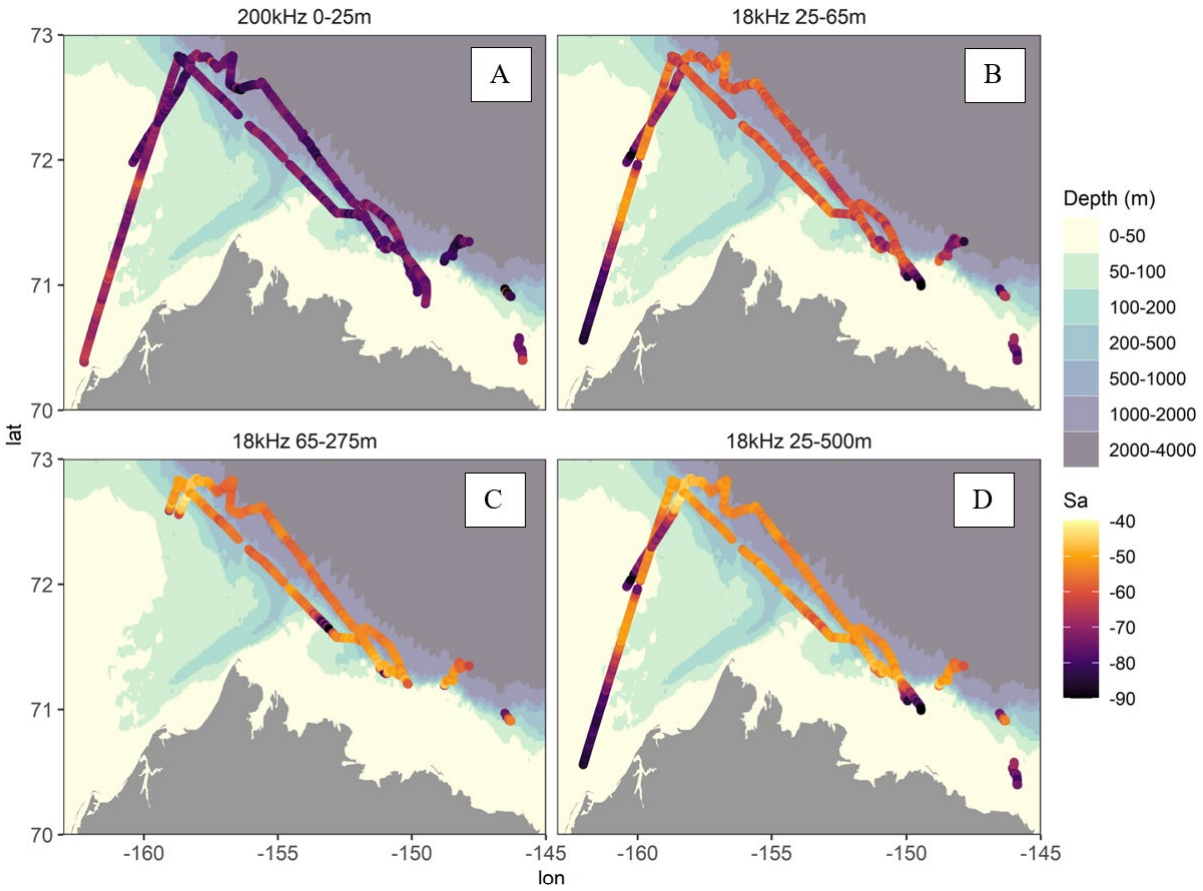

Figure 27: Backscattering strength (S_a in dB) integrated along the survey for (A) the 10–25 m layer at 200 kHz; (B) the 25–65 m layer at 18 kHz; (C) the 65v275 m layer at 18 kHz; and (D) the 25–500 m layer at 18 kHz. For similar organisms, a higher S_a indicates higher abundance. Spatial resolution is 0.25 nm.

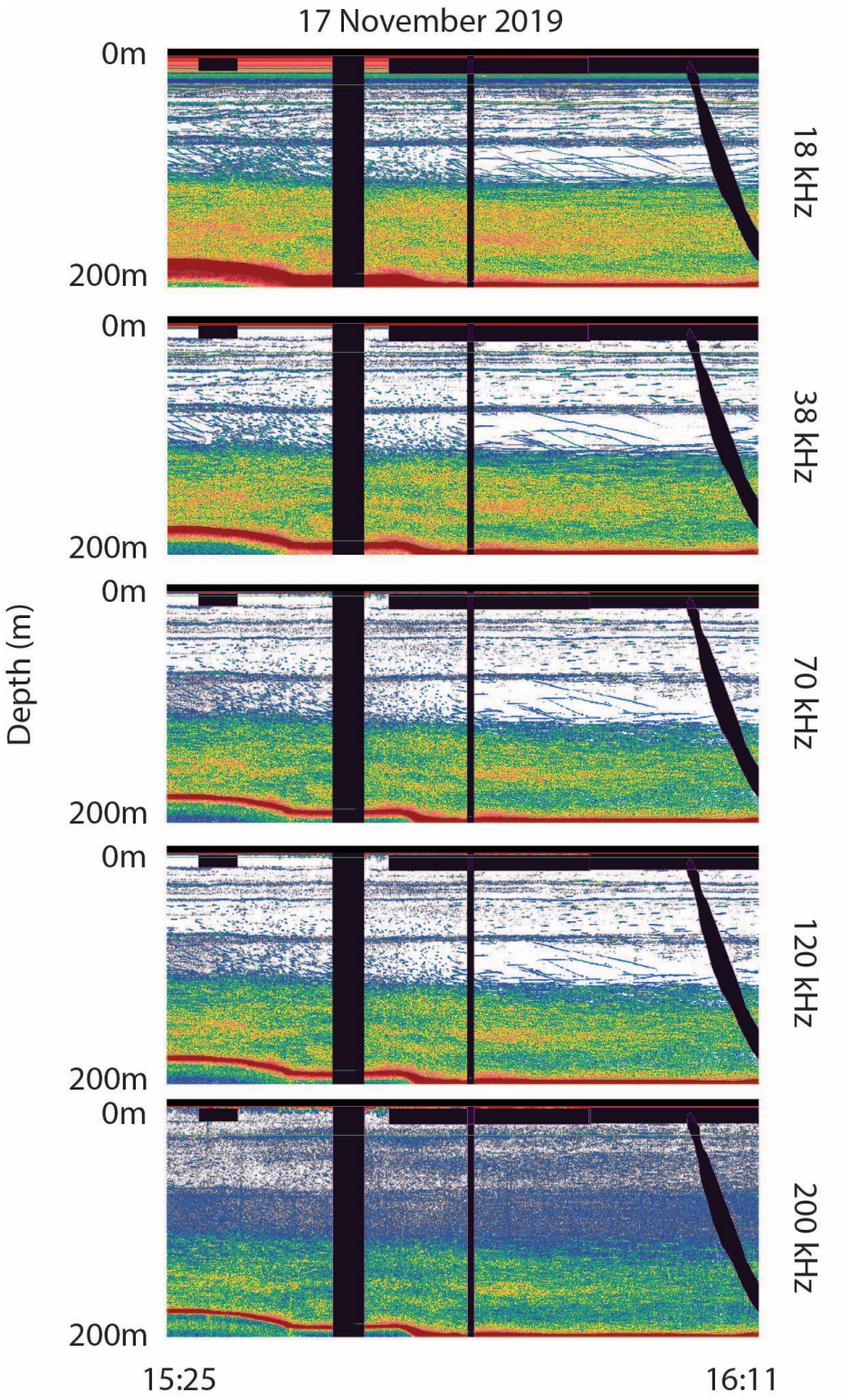

Figure 28: S_v echograms showing a dense layer of fish above the bottom in a 200 m depth region on 17 November. The thick red line indicates the seafloor, and the black areas indicate no data. The color scale varies from -90 to -40 dB.

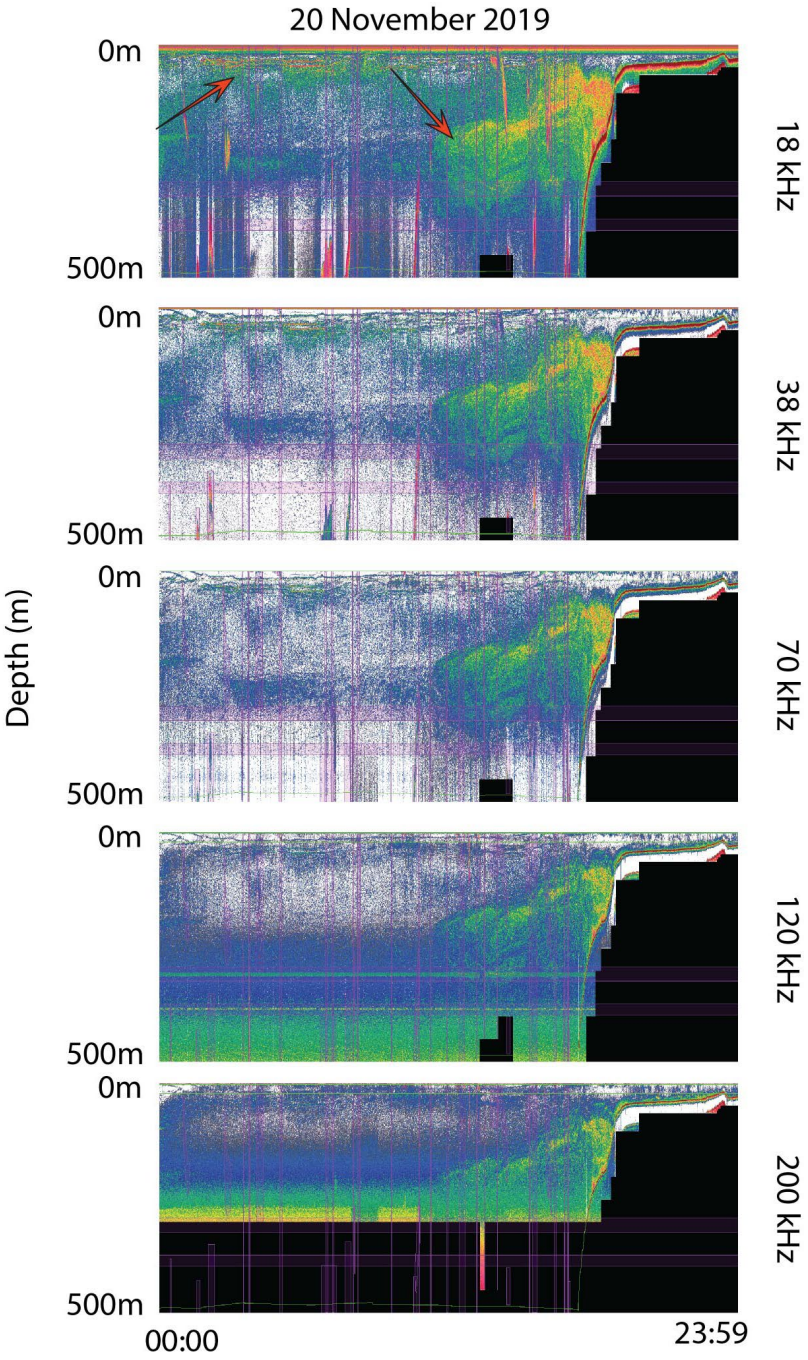

Figure 29: S_v echograms for the entire day of 20 November. The arrows indicate the ascent and descent of smaller organisms from the deeper SSL. Note the dense school above the shelf break. Black areas indicate no data. The color scale varies from -90 to -40 dB.

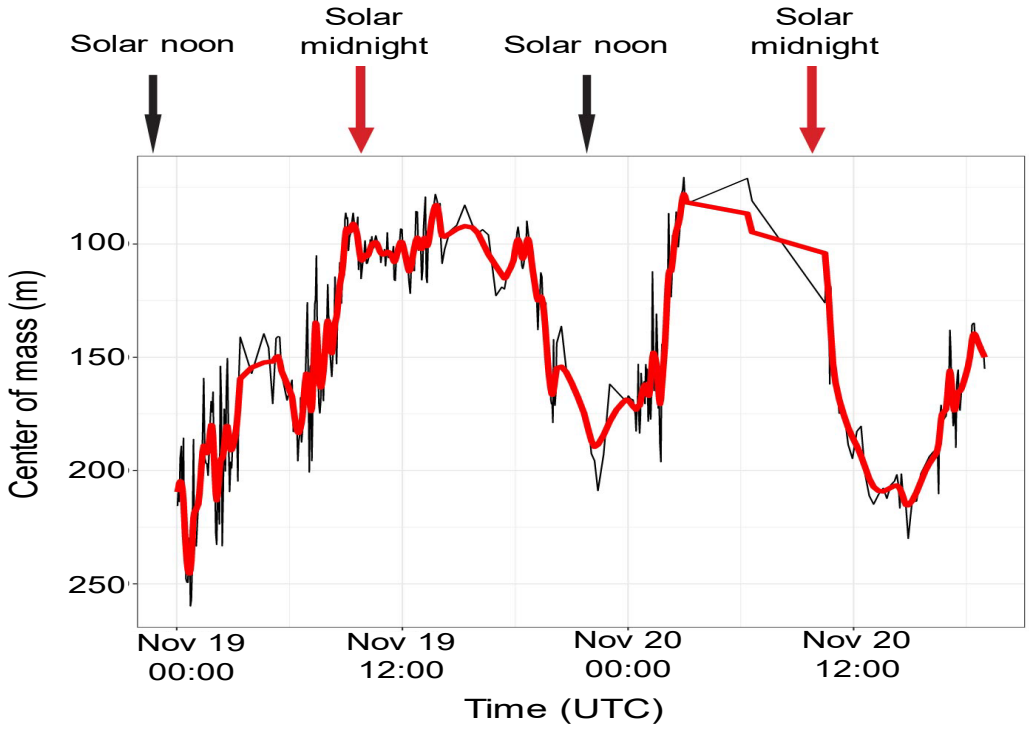

Figure 30: Variation in center of mass on 19–20 November (black line). The red line indicates a Gaussian kernel smoothed over 10 values.

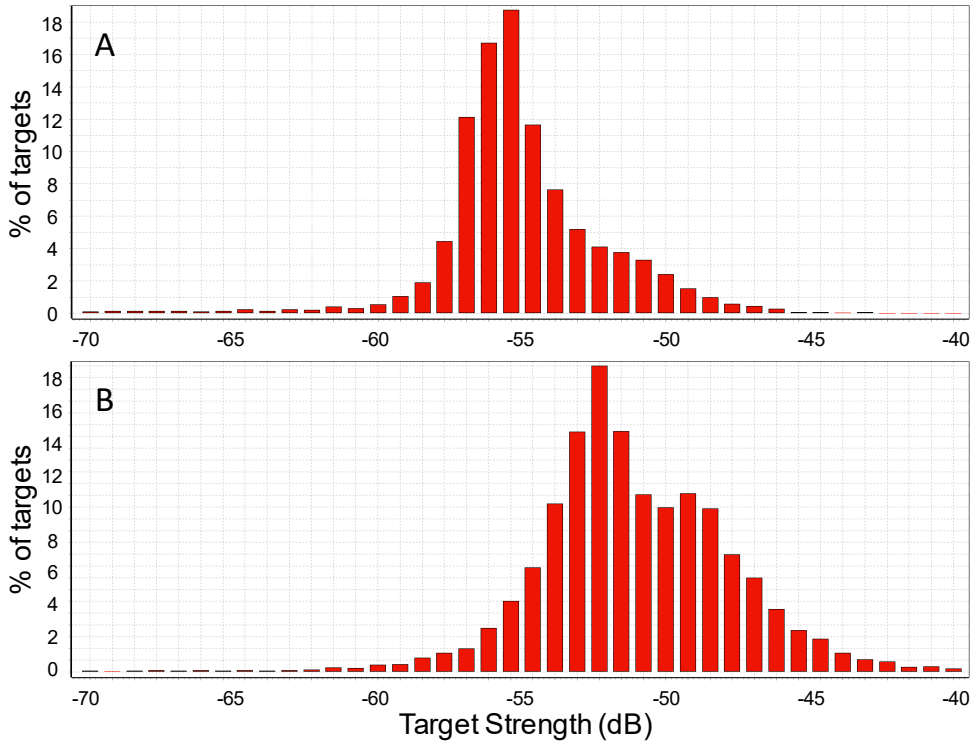

Figure 31: Histograms of target strength distribution in (A) the top migrating layer and (B) the deep SSL around 07:00 UTC on November 20.

DISCUSSION

The overall goal of this study was to assess how Arctic cod utilize habitats under young sea ice in the fall. We documented a close association between juvenile Arctic cod and newly formed sea ice throughout our study region along the continental slope from the Chukchi Sea to the eastern Beaufort Sea. The observed densities of Arctic cod (Table 2) were at least an order of magnitude lower than the average density on the seafloor of the Northeast Chukchi Sea shelf during late summer (36,811 individuals per km^2; Mueter *et al.*, 2021). However, densities were comparable to those observed under older and thicker sea ice (45 – 140 cm) sampled during summer of 2012 in the Eurasian Basin of the Arctic, which averaged 5,352 individuals per km^2 (David et al., 2016). Thus, our primary hypothesis, that young Arctic cod are associated with newly-formed sea ice, was clearly supported.

Arctic cod associating with the newly formed sea ice, based on their size distribution, likely included both young-of-year and older (age 1+) fish. About 2/3 of the Arctic cod stomachs contained undigested or partially digested food items, implying that Arctic cod were actively feeding on a variety of prey items, including both sea ice-associated and water-column zooplankton (Figure 17, Table 4). Moderate densities of zooplankton were available in the water column, including common prey items such as *Calanus glacialis*, *Metridia longa,* and other calanoid copepods (Figure 6). On-board observations and respirometry experiments (unpublished data) suggested that both *C. glacialis* and *M. longa* were metabolically active. Large lipid droplets were evident in all *C. glacialis* individuals, indicating good feeding conditions during previous months. Although *C. glacialis* is widely believed to enter seasonal diapause in late summer, their continued presence in the water column in mid-November (Figure 6) and active metabolic status clearly show that they remained active along the outer shelf and slope of the Chukchi and Beaufort seas at least into late November 2019. This, and their observed prevalence in Arctic cod diets (Figure 17), suggests that calanoid copepods may provide an important late-season food source for juvenile Arctic cod as they enter winter. Evidence of diel vertical migration of small Arctic cod from the acoustic survey (Figure 29, Figure 30) also supports the notion that Arctic cod are actively feeding on zooplankton in the upper water column as DVM is generally associated with a trade-off between feeding and avoiding predators (Kaartvedt *et al*., 1996).

In addition to mesozooplankton prey in the water column (Figure 6), larger zooplankton such as juvenile hyperiids (*Themisto libellula*), ice amphipods (*Onisimus* spp., *Eusirus holmii, Apherusa glacialis*), krill (*Thysanoessa raschii* and *T. inermis*) and nearshore mysids (*Neomysis rayii*, *Acanthomysis pseudomacropsis*) were sometimes abundant at the sea ice-water interface as suggested by qualitative SUIT hauls. Several of these larger zooplankton species were common in Arctic cod diets (e.g., *A. glacialis*, *N. rayii*), although it is unclear if they were consumed at the ice-water interface or in the water column. The limited sampling of larger zooplankton in the water column (Methot trawl, n=2) showed a notable difference in the species composition of large zooplankton between one open-water station and one under-ice station (Figure 8). In particular, the open water station was dominated by krill, whereas krill were uncommon at the under-ice station (020). The open-water station was located downstream from Barrow Canyon, a known hotspot for krill, and was one of three stations (006, 020, 021) where Arctic cod had consumed krill (Maes 2022).

Our results imply that at least some fraction of juvenile Arctic cod associated with newly formed sea ice in the fall of 2019; however, a lack of density estimates for the water column makes it difficult to assess the importance of sea-ice habitat for Arctic cod in the fall. Although sea ice may provide both food and shelter for Arctic cod, the newly formed ice in November offered little structure for shelter, and juveniles

likely rose to the ice to supplement their diet with ice-associated zooplankton, which is consistent with acoustic backscatter evidence showing DVM extended to very near the surface (Figure 29). This behavior may reflect a strategy that could provide energetically rich prey at a time when most individuals captured under the ice appeared to be in poor condition, with lipid densities that were associated with high mortalities under starvation conditions in the laboratory (Figure 21). This poor energetic condition may have been the result of unusually warm temperatures in the region. Chukchi Sea temperatures in 2019 were the highest recorded since 2007, which had the warmest temperatures in the satellite record (Timmermans and Labe, 2022). Young Arctic cod have a unique lipid-storage strategy where high lipid levels are associated with diatom- and *Calanus*-sourced fatty acids and reduced lipid content is associated with elevated temperatures (Copeman *et al.*, 2022b). Compared to earlier years, Arctic cod on the Chukchi Sea shelf in 2019 were confined to a smaller region in the Northeast Chukchi Sea and occurred at warmer average temperatures (Copeman *et al.*, 2022b). Although they had higher lipid storage in the region in late summer 2019 compared to 2017 (Copeman *et al.*, 2022b), warm temperatures and reduced *Calanus glacialis* abundances in the Chukchi Sea in 2019 may have led to the inability to maintain high lipid reserves between late summer and fall.

Arctic cod in this study were found along the entire slope region from the westernmost station in the Chukchi Sea to the eastern Beaufort Sea (Figure 9). Arctic cod were found both in association with the ice and in the underlying water column. While acoustic backscatter suggested a patchy distribution on the Chukchi Sea shelf, fish were distributed in near-continuous layers along much of the slope (Figures 25–27). While juvenile and older Arctic cod have previously been documented along much of the Beaufort Sea slope (Parker-Stetter *et al.*, 2011; Majewski *et al.*, 2013; Geoffroy *et al.*, 2016), no sign of mid-water fish was evident during a transect across the Chukchi Sea slope in 2013 (De Robertis *et al.*, 2017). As observed in similar studies in the Canadian Beaufort Sea (Benoit *et al.*, 2014; Geoffroy *et al.*, 2016), Arctic cod were vertically separated into a deep layer, likely consisting of larger and older fish, and shallower dispersed layers composed of smaller juveniles (Figures 26, 28, 29, 31). Small Arctic cod (≥3.5 cm) leave the epipelagic layer in late summer and fall to descend to deeper waters while still conducting DVM to feed (Geoffroy *et al.*, 2016). Our results suggest that these feeding movements continue at least into late November (Figure 30). Zooplankton backscatter was still evident in the top 25 m at the onset of winter (Figure 24), consistent with moderate densities of net-sampled zooplankton at discrete stations (Figure 6), and smaller Arctic cod were most likely feeding on zooplankton during nighttime, as suggested by diet compositions.

Although we are uncertain about the origins of Arctic cod observed in this study, the source region is likely to be in the Chukchi Sea as our study area along the Beaufort and Chukchi slopes are downstream from and connected to the Chukchi shelf via Barrow Canyon (Figure 1). Large concentrations of first-year Arctic cod use the Northeast Chukchi Shelf as a nursery area (De Robertis *et al.*, 2017) and are likely transported off the shelf through Barrow Canyon in late summer and fall (Levine *et al.*, 2021). Shelf waters exit Barrow Canyon either eastward with the Beaufort slope current or westward with the Chukchi slope current (Corlett and Pickart, 2017; Weingartner *et al.*, 2017). In November 2019, warmer and saltier shelf waters with slightly elevated nutrient concentrations were evident at station 006 to the east of Barrow Canyon as well as station 030 just off the mouth of Barrow Canyon, suggesting that Arctic cod at these stations originated on the Chukchi Sea shelf and were advected via Barrow Canyon. It is possible that Arctic cod collected at stations to the east or west of Barrow Canyon may have originated elsewhere.

Previous analyses have suggested the population structure of Arctic cod within the Alaskan Arctic. The discontinuous distribution of juvenile Arctic cod (Forster *et al.*, 2020), differences in hatch dates and larval growth rates (Chapman *et al.*, 2023), differences in otolith microchemistry (Chapman 2021), and genetic analyses (Wilson *et al.*, 2019, 2020; Nelson *et al.*, 2020) all point to at least two distinct populations. A Chukchi Sea population, extending into the western Beaufort Sea, likely originates from multiple separate spawning areas and events in the northern Bering Sea, the Bering Strait region, and Kotzebue Sound (Deary *et al.*, 2021; Vestfals *et al.*, 2021). These appear to be separated from Arctic cod in the eastern Beaufort Sea that may originate from spawning aggregations in the Canadian Beaufort Sea such as those observed in Franklin Bay (Benoit *et al.*, 2008). Two separate populations are consistent with the genetic differentiation between the Chukchi Sea and Beaufort Sea samples collected in this study, although further analyses by station will be needed to see if these differences reflect an east-west gradient or two distinct groups (Figure 16). Arctic cod at our easternmost locations (stations 020, 021, 022) may have originated farther east in the Canadian Beaufort Sea, whereas Arctic cod sampled along the Chukchi Sea slope originated on the Chukchi Sea shelf. However, Arctic cod at station 006, which were part of the Beaufort Sea group in genetic analyses (Figure 16), likely originated in the Chukchi Sea as the water mass characteristics at this station are more similar to Chukchi Sea water (Figure 3).

The samples collected during this study contributed to several studies on Arctic cod at pan-Arctic scales, including a study comparing the Arctic cod gut microbiome between the Atlantic and Pacific Arctic (Maes 2022), and genetic analyses of Arctic cod population structure across the Arctic (Maes 2022, Figures 14–16). The microbiome study was the first study to establish an ecological baseline of bacterial diversity in the gut microbiome of Arctic cod, documenting a diverse community of bacteria including many unknown sequences. Improved baselines will be needed to fully resolve the microbiome and monitor bacterial communities in the Arctic over time.

CONCLUSIONS

Our study has shown that at least some Arctic cod in the Pacific Arctic associate with newly formed sea ice to supplement their diets with sea ice-associated zooplankton prey. Suitable prey for Arctic cod, including high-lipid calanoid copepods, were also available in the water column below the ice at low to moderate abundances. In fact, diets were dominated by water column zooplankton, suggesting that Arctic cod may be loosely associated with the sea ice at this time of year, feeding opportunistically on available prey at the ice-water interface and throughout the water column. The availability of suitable prey may enable Arctic cod to put on additional lipid reserves even in late November. However, Arctic cod collected at the sea-ice/water interface during November 2019 were in poor energetic condition and it is unclear if they would have been able to obtain sufficient prey to survive their first winter. Comparisons between juvenile fish sampled in the preceding summer and those caught in November suggest that Arctic cod may have depleted their energy reserves between September and November, possibly as a result of elevated metabolic rates associated with unusually high water temperatures. While some studies have suggested that Arctic cod may initially benefit from increasing temperatures due to an extended growing season (Bouchard *et al.*, 2017), warmer temperatures and reduced abundances of *Calanus glacialis* may result in reduced lipid storage (Copeman *et al.*, 2022b) and may ultimately compromise overwinter survival, as suggested by the poor condition of Arctic cod sampled under the sea ice in this study.

This study demonstrated the utility of the Surface- and Under-Ice Trawl for sampling under-ice fauna from an ice-capable vessel, *R/V Sikuliaq*, and represents the first successful deployment of a SUIT in the Pacific Arctic. While deployments were not without challenges, we were able to quantify the density of

Arctic cod at the ice-water interface (upper 2 m) and show their increasing use of the ice-water interface as sea-ice thickness increases. At the same time, we were able to assess the vertical distribution of fish, presumably Arctic cod, in the upper 500 m of the water column and show that they were widely distributed throughout the study area and were likely vertically segregated by size with dense aggregations of larger fish distributed at 100–250 m, impinging on the upper slope of the Chukchi and Beaufort seas just below the shelf break (Figure 29). However, we were unable to assess the relative abundance of Arctic cod under the ice compared to the water column as we currently lack reliable estimates of the density of fish in the water column, which requires sampling aggregations of fish under the ice.

ACKNOWLEDGMENTS

We are grateful to the University of Alaska Fairbanks (UAF), College of Fisheries and Ocean Sciences for authorizing Alpha Helix funds to support the purchase of a Surface and Under-Ice Trawl (SUIT) that made this study possible. We thank the Arctic Icebreaker Research Consortium and UAF for providing ship time on *R/V Sikuliaq* for under-ice sampling in November 2019. The UAF team (Franz Mueter, Alexei Pinchuk, and Jared Weems), zooplankton analyses, and lipid analyses were supported by the Alaska Coastal Marine Institute and the Bureau of Ocean Energy Management (cooperative agreement M19AC00018). We are deeply indebted to Jim Thompson at the University of Washington (UW) and the Coastal Ocean Dynamics in the Arctic (CODA) project crew, who were willing to spend an additional week at sea under challenging conditions to support our work. The CODA participants were funded by the National Science Foundation Office of Polar Programs and Ocean Sciences (award 1818485 to Dr. Thomson of UW, and award 1913195 to Dr. Eidam of the University of North Carolina). We could not have done this work without the incredible dedication of the captain, crew, and marine technicians onboard *R/V Sikuliaq*, who worked tirelessly to support the science. Their efforts underpin everything achieved during this research cruise. The National Ice Center (NIC) provided essential ice charting products daily, which were used for safe navigation and for targeting science measurements. We thank all CODA and Go-West cruise participants for their support in the field. Analysis of acoustic data was supported by the Fisheries and Marine Institute at Memorial University. Genetic analyses were supported by a Brilliant Marine Research Idea Philanthropy Award 2019 issued by Flanders Marine Institute, Belgium, to Sarah Maes and by the Catholic University of Leuven.

STUDY PRODUCTS

Sarah Maes (2022). Population genomics and trophic ecology of polar cod (*Boreogadus saida*) in a changing Arctic Ocean. Ph.D. Thesis, Catholic University of Leuven (KUL).

Chapman, Zane (2021). Otolith derived hatch dates, growth rates, and microchemistry of Arctic cod (*Boreogadus saida*) support the existence of several spawning populations in Alaskan waters. MS thesis. University of Alaska Fairbanks.

Chapman, Z. M., Mueter, F. J., Norcross, B. L., and Oxman, D. S. 2023. Arctic cod (*Boreogadus saida*) hatching season and growth rates in the Bering, Chukchi and Beaufort seas. Deep Sea Research II, 207: 105226. https://doi.org/10.1016/j.dsr2.2022.105226.

Publications in Progress

Sarah M. Maes, Henrik Christiansen, Caroline Bouchard, Enora Geslain, Bart Hellemans, Felix C. Mark, Magnus Lucassen, Franz Mueter, Filip. A.M. Volckaert, Hauke Flores. The circumpolar population structure and connectivity of polar cod (*Boreogadus saida*).

Sarah M. Maes, Alexei Pinchuk, Henrik Christiansen, Bart Hellemans, Franz Mueter, Filip A.M. Volckaert, Hauke Flores. The diet of sea ice-associated polar cod in the Alaskan Arctic Ocean during autumn.

Sarah M. Maes, Henrik Christiansen, Bart Hellemans, Magnus Lucassen, Franz Mueter, Hauke Flores, Filip A.M. Volckaert. Diversity of the gut microbiome of polar cod across the Arctic Ocean.

Additionally, a synthesis manuscript based on the results presented in this report is in preparation but was delayed considerably due to the challenges of collaborating across laboratories in Europe and the US during the COVID pandemic. We expect to submit a manuscript by mid-2023.

Presentations

Mueter, F.J., Pinchuk, A., Copeman, L., Maes, S., Geoffroy, M., Chapman, Z. Weems, J., Flores, H. Arctic Cod (*Boreogadus saida*) under newly-formed sea ice in the Pacific Arctic. Ecosystem Studies of the Subarctic and Arctic Seas (ESSAS) Annual Science Meeting, Seattle, WA, June 20–22, 2022.

Mueter, F.J., Pinchuk, A., Copeman, L., Maes, S., Geoffroy, M., Chapman, Z. Weems, J., Flores, H. Arctic Cod (*Boreogadus saida*) under newly-formed ice. Coastal Marine Institute Annual Research Review, Virtual meeting, January 19, 2022.

Chapman, Zane M. Otolith-derived hatch dates, growth rates, and microchemistry of Arctic cod (*Boreogadus saida*) support the existence of several spawning populations in Alaskan waters. Thesis defense and public seminar, University of Alaska Fairbanks, Juneau, AK, March 29, 2021.

Mueter, F.J., J.M. Grebmeier, J.M., H.P. Huntington, P.L. Pulsifer, J. Davis. A Step-Wise Progression to Fisheries Ecosystem Science in the Central Arctic. [Including references to under-ice sampling during the Go-West cruise]. Arctic Science Summit Week, Virtual meeting, March 26, 2021.

Mueter, F.J., J. Marsh, C. Vestfals, R. Levine, A. de Robertis, GO-WEST team. Fisheries studies, with a focus on Arctic cod (*Boreogadus saida*), in the Pacific Arctic. IARPC (Interagency Arctic Research Policy Committee) Marine Ecosystems collaboration team webinar, March 25, 2020.

Mueter, F. J., H. Flores, A. Pinchuk, J. Weems, R. ten Boer, M. van Dorssen, L. Edenfield, A. Klasmeier, K. Kunz, S. Maes, N. Zakharova. Chasing Arctic cod under the ice. Strait Science (UAF seminar series), Nome, AK, March 11, 2020.

Mueter, F. J., H. Flores, A. Pinchuk, J. Weems, R. ten Boer, M. van Dorssen, L. Edenfield, A. Klasmeier, K. Kunz, S. Maes, N. Zakharova. Utilization of the under-ice habitat by Arctic Cod in the western Arctic Ocean: Chasing fish under ice. CMI Annual Research Review, Anchorage, AK, January 31, 2020.

REFERENCES

Ajiad, A. M., Oganin, I. A., and Gjøsæter, H. 2011. Polar cod. pp. 315–328 *In* Thee Barents Sea. Ecosystem, Resources, Management. Half a Century of Russian-Norwegian Cooperation. Edited by T. Jakobsen and V. K. Ozhigin. Tapir Academic Press, Trondheim, NO.

Altukhov, K. A. 1981. The reproduction and development of the Arctic cod, *Boreogadus saida*, in the White Sea. Journal of Ichthyology, 19: 93–101.

Benoit, D., Simard, Y., and Fortier, L. 2008. Hydroacoustic detection of large winter aggregations of Arctic cod (Boreogadus saida) at depth in ice-covered Franklin Bay (Beaufort Sea). Journal of Geophysical Research, 113: C06S90.

Benoit, D., Simard, Y., Gagne, J., Geoffroy, M., and Fortier, L. 2010. From polar night to midnight sun: photoperiod, seal predation, and the diel vertical migrations of polar cod (*Boreogadus saida*) under landfast ice in the Arctic Ocean. Polar Biology, 33: 1505–1520.

Benoit, D., Simard, Y., and Fortier, L. 2014. Pre-winter distribution and habitat characteristics of polar cod (*Boreogadus saida*) in the southeastern Beaufort Sea. Polar Biology, 37: 149–163. https://doi.org/10.1007/s00300-013-1419-0.

Bluhm, B. A., and Gradinger, R. 2008. Regional variability in food availability for arctic marine mammals. Ecological Applications, 18: S77–S96.

Boitsov, V. D., Dolgov, A. V, Krysov, A. I., Seliverstova, E. I., and Shevelev, M. S. 2013. Polar cod of the Barents Sea. PINRO Press, Murmansk (In Russian).

Borkin, L. V, Ozhigin, V. K., and Shleinik, V. N. 1987. Effect of oceanographical factors on the abundance of the Barents Sea polar cod year classes. pp. 169–180 *In* The Effect of Oceanographic Conditions on Distribution and Population Dynamics of Commercial Fish Stocks in the Barents Sea: Proceedings of the Third Soviet-Norwegian Symposium, Murmansk, 26–28 May 1986. Edited by H. Loeng. Institute of Marine Research, Bergen, NO.

Bouchard, C., and Fortier, L. 2011. Circum-arctic comparison of the hatching season of polar cod *Boreogadus saida*: A test of the freshwater winter refuge hypothesis. Progress In Oceanography, 90: 105–116.

Bouchard, C., Geoffroy, M., LeBlanc, M., Majewski, A., Gauthier, S., Walkusz, W., Reist, J. D., *et al.* 2017. Climate warming enhances polar cod recruitment, at least transiently. Progress in Oceanography, 156: 121–129.

Bouchard, C., Charbogne, F. Baumgartner and S. M. Maes. 2020. West Greenland ichthyoplankton and how melting glaciers could allow Arctic cod larvae to survive extreme summer temperatures. Arctic Science 7(1): 217-239

Callahan, B. J., McMurdie, P. J., and Holmes, S. P. 2017. Exact sequence variants should replace operational taxonomic units in marker-gene data analysis. The ISME Journal, 11: 2639–2643. https://doi.org/10.1038/ismej.2017.119.

Chapman, Z. M. 2021. Otolith derived hatch dates, growth rates, and microchemistry of Arctic cod (*Boreogadus saida*) support the existence of several spawning populations in Alaskan waters. University of Alaska Fairbanks. 84 pp.

Chapman, Z. M., Mueter, F. J., Norcross, B. L., and Oxman, D. S. 2023. Arctic cod (*Boreogadus saida*) hatching season and growth rates in the Bering, Chukchi and Beaufort seas. Deep Sea Research II, 207: 105226. https://doi.org/10.1016/j.dsr2.2022.105226.

Copeman, L. A., Laurel, B. J., Boswell, K. M., Sremba, A. L., Klinck, K., Heintz, R. A., Vollenweider, J. J., *et al.* 2016. Ontogenetic and spatial variability in trophic biomarkers of juvenile saffron cod (*Eleginus gracilis*) from the Beaufort, Chukchi, and Bering Seas. Polar Biology, 39: 1109–1126.

Copeman, L. A., Laurel, B. J., Spencer, M., and Sremba, A. 2017. Temperature impacts on lipid allocation among juvenile gadid species at the Pacific Arctic-Boreal interface: an experimental laboratory approach. Marine Ecology Progress Series, 566: 183–198. https://doi.org/ 10.3354/meps12040.

Copeman, L. A., Stowell, M. A., Salant, C. D., Ottmar, M. L., Spencer, M. L., Iseri, P. J., and Laurel, B. J. 2022a. The role of temperature on overwinter survival, condition metrics, and lipid loss in juvenile polar cod (*Boreogadus saida*): A laboratory experiment. Deep Sea Research Part II: Topical Studies in Oceanography, 205: 105177. https://doi.org/10.1016/j.dsr2.2022.105177.

Copeman, L. A., Salant, C. D., Stowell, M. A., Spencer, M. L., Kimmel, D. G., Pinchuk, A. I., and Laurel, B. J. 2022b. Annual and spatial variation in the condition and lipid storage of juvenile Chukchi Sea gadids during a recent period of environmental warming (2012–2019). Deep Sea Research Part II: Topical Studies in Oceanography, 205: 105177. https://doi.org/10.1016/j.dsr2.2022.105177.

Corlett, W. B., and Pickart, R. S. 2017. The Chukchi slope current. Progress in Oceanography, 153: 50–65. https://doi.org/10.1016/j.pocean.2017.04.005.

Coyle, K. O., and Pinchuk, A. I. 2002. Climate-related differences in zooplankton density and growth on the inner shelf of the southeastern Bering Sea. Progress in Oceanography, 55: 177–194. https://doi.org/10.1016/S0079-6611(02)00077-0.

Darnis, G., Hobbs, L., Geoffroy, M., Grenvald, J. C., Renaud, P. E., Berge, J., Cottier, F., *et al.* 2017. From polar night to midnight sun: Diel vertical migration, metabolism and biogeochemical role of zooplankton in a high Arctic fjord (Kongsfjorden, Svalbard). Limnology and Oceanography, 62: 1586–1605. https://doi.org/10.1002/lno.10519.

David, C., Lange, B., Krumpen, T., Schaafsma, F., van Franeker, J. A., and Flores, H. 2016. Under-ice distribution of polar cod *Boreogadus saida* in the central Arctic Ocean and their association with sea-ice habitat properties. Polar Biology, 39: 981–994.

De Robertis, A., and Higginbottom, I. 2007. A post-processing technique to estimate the signal-to-noise ratio and remove echosounder background noise. ICES Journal of Marine Science, 64: 1282–1291. https://doi.org/10.1093/icesjms/fsm112.

De Robertis, A., Taylor, K., Wilson, C. D., and Farley, E. V. 2017. Abundance and distribution of Arctic cod (Boreogadus saida) and other pelagic fishes over the U.S. continental shelf of the northern Bering and Chukchi seas. Deep Sea Research Part II: Topical Studies in Oceanography, 135: 51–65.

Deary, A. L., Vestfals, C. D., Mueter, F. J., Logerwell, E. A., Goldstein, E. D., Stabeno, P. J., Danielson, S. L., *et al.* 2021. Seasonal abundance, distribution, and growth of the early life stages of polar cod (Boreogadus saida) and saffron cod (Eleginus gracilis) in the US Arctic. Polar Biology, 44: 2055–2076. https://doi.org/10.1007/s00300-021-02940-2.

Demer, D. A., Berger, L., Bernasconi, M., Demer, D. A., Berger, L., Bernasconi, M., Bethke, E., *et al.* 2015. Calibration of acoustic instruments. 133 pp. https://doi.org/10.25607/OBP-185.

Flores, H., van Franeker, J. A., Siegel, V., Haraldsson, M., Strass, V., Meesters, E. H., Bathmann, U., *et al.* 2012. The Association of Antarctic Krill *Euphausia superba* with the Under-Ice Habitat. PLoS One, 7: e31775. https://doi.org/10.1371/journal.pone.0031775.

Folch, J., Less, M., and Sloane Stanley, G. H. 1957. A simple method for the isolation and purification of total lipids from animal tissues. Journal of Biological Chemistry, 226: 497–509.

Forster, C. E., Norcross, B. L., Mueter, F. J., Logerwell, E. A., and Seitz, A. C. 2020. Spatial patterns, environmental correlates, and potential seasonal migration triangle of polar cod (*Boreogadus saida*) distribution in the Chukchi and Beaufort seas. Polar Biology, 43: 1073–1094. https://doi.org/10.1007/s00300-020-02631-4.

Geoffroy, M., Robert, D., Darnis, G., and Fortier, L. 2011. The aggregation of polar cod (*Boreogadus saida*) in the deep Atlantic layer of ice-covered Amundsen Gulf (Beaufort Sea) in winter. Polar Biology, 34: 1959–1971. https://doi.org/10.1007/s00300-011-1019-9.

Geoffroy, M., Majewski, A., LeBlanc, M., Gauthier, S., Walkusz, W., Reist, J. D., and Fortier, L. 2016. Vertical segregation of age-0 and age-1+ polar cod (*Boreogadus saida*) over the annual cycle in the Canadian Beaufort Sea. Polar Biology, 39: 1023–1037. https://doi.org/10.1007/s00300-015-1811-z.

Gillispie, J. G., Smith, R. L., Barbour, E., and Barber, W. E. 1997. Distribution, abundance, and growth of Arctic cod in the northeastern Chukchi Sea. pp. 81-89, In J.B. Reynolds (ed.) Fish ecology in Arctic North America. American Fisheries Society Symposium 19, Fairbanks, AK.

Gordon, L. I., Jennings, J. C., Ross, A. A., and Krest, J. M. 1993. A suggested protocol for continuous flow analysis of seawater nutrients (phosphate, nitrate, nitrite, and silicic acid) in the WOCE Hydrographic Program and the Joint Global Ocean Fluxes Study. WOCE Hydrographic Program Office, Methods Manual WHPO, 91–100.

Gradinger, R. R., and Bluhm, B. A. 2004. In-situ observations on the distribution and behavior of amphipods and Arctic cod (*Boreogadus saida*) under the sea ice of the High Arctic Canada Basin. Polar Biology, 27: 595–603. https://doi.org/10.1007/s00300-004-0630-4.

Gray, B. P., Norcross, B. L., Blanchard, A. L., Beaudreau, A. H., and Seitz, A. C. 2016. Variability in the summer diets of juvenile polar cod (*Boreogadus saida*) in the northeastern Chukchi and western Beaufort Seas. Polar Biology, 39: 1069–1080.

Handy, S. M., Deeds, J. R., Ivanova, N. V, Hebert, P. D. N., Hanner, R. H., Ormos, A., Weigt, L. A., *et al.* 2011. A Single-Laboratory Validated Method for the Generation of DNA Barcodes for the Identification of Fish for Regulatory Compliance. Journal of AOAC INTERNATIONAL, 94: 201–210. https://doi.org/10.1093/jaoac/94.1.201.

Harter, B. B., Elliott, K. H., Divoky, G. J., and Davoren, G. K. 2013. Arctic Cod (*Boreogadus saida*) as Prey: Fish length-energetics relationships in the Beaufort Sea and Hudson Bay. Arctic, 66: 191–196.

Hop, H., and Gjøsæter, H. 2013. Polar cod (*Boreogadus saida*) and capelin (*Mallotus villosus*) as key species in marine food webs of the Arctic and the Barents Sea. Marine Biology Research, 9: 878–894.

Hunt, G. L., Ressler, P. H., Gibson, G. A., De Robertis, A., Aydin, K., Sigler, M. F., Ortiz, I., *et al.* 2016. Euphausiids in the eastern Bering Sea: A synthesis of recent studies of euphausiid production, consumption and population control. Deep Sea Research Part II: Topical Studies in Oceanography, 134: 204–222. http://www.sciencedirect.com/science/article/pii/S0967064515003380.

Jombart, T., Devillard, S., and Balloux, F. 2010. Discriminant analysis of principal components: a new method for the analysis of genetically structured populations. BMC Genetics, 11: 94. https://doi.org/10.1186/1471-2156-11-94.

Kaartvedt, S., Melle, W., Knutsen, T., and Skjoldal H. R. 1996. Vertical distribution of fish and krill beneath water of varying optical properties. Marine Ecology Progress Series, 136: 51–58. http://doi.org/10.3354/meps136051

Kohlbach, D., Graeve, M., Lange, B., David, C., Peeken, I., and Flores, H. 2016. The importance of ice algae-produced carbon in the central Arctic Ocean ecosystem: Food web relationships revealed by lipid and stable isotope analyses. Limnology and Oceanography, 61: 2027–2044. http://dx.doi.org/10.1002/lno.10351.

Kohlbach, D., Schaafsma, F. L., Graeve, M., Lebreton, B., Lange, B. A., David, C., Vortkamp, M., *et al.* 2017. Strong linkage of polar cod (*Boreogadus saida*) to sea ice algae-produced carbon: Evidence from stomach content, fatty acid and stable isotope analyses. Progress in Oceanography, 152: 62–74. http://www.sciencedirect.com/science/article/pii/S0079661116301495.

Leu, E., Søreide, J. E. E., Hessen, D. O. O., Falk-Petersen, S., and Berge, J. 2011. Consequences of changing sea-ice cover for primary and secondary producers in the European Arctic shelf seas: Timing, quantity, and quality. Progress in Oceanography, 90: 18–32. https://doi.org/10.1016/j.pocean.2011.02.004.

Levine, R. M., De Robertis, A., Grünbaum, D., Woodgate, R., Mordy, C. W., Mueter, F., Cokelet, E., *et al.* 2021. Autonomous vehicle surveys indicate that flow reversals retain juvenile fishes in a highly advective high-latitude ecosystem. Limnology and Oceanography, 66: 1139–1154. https://doi.org/10.1002/lno.11671.

Lønne, O. J., and Gulliksen, B. 1989. Size, age and diet of polar cod, *Boreogadus saida* (Lepechin 1773), in ice covered waters. Polar Biology, 9: 187–191. https://doi.org/10.1007/BF00297174.

Lowry, L. F., and Frost, K. J. 1981. Distribution, Growth, and Foods of Arctic Cod (*Boreogadus saida*) in the Bering, Chukchi, and Beaufort Seas. Canadian Field-Naturalist, 95: 186–191.

Lu, Y., Ludsin, S. A., Fanslow, D. L., and Pothoven, S. A. 2008. Comparison of three microquantity techniques for measuring total lipids in fish. Canadian Journal of Fisheries and Aquatic Sciences, 65: 2233–2241. https://doi.org/10.1139/F08-135.

Maes, S. 2022. Population genomics and trophic ecology of polar cod (*Boreogadus saida*) in a changing Arctic Ocean. Ph.D. thesis, Catholic University of Leuven (KUL), Leuven, BE.

Maes, S. M., Schaafsma, F. L., Christiansen, H., Hellemans, B., Lucassen, M., Mark, F. C., Flores, H. M., *et al.* 2022. Comparative visual and DNA-based diet assessment extends the prey spectrum of polar cod *Boreogadus saida*. Marine Ecology Progress Series, 698: 139–154. https://doi.org/10.3354/meps14145.

Magdanz, J. S., Braem, N. S., Robbins, B. S., and Koster, D. S. 2010. Subsistence harvests in Northwest Alaska, Kivalina, and Noatak, 2007. Alaska Department of Fish and Game Division of Subsistence Technical Paper No. 354, Kotzebue, AK.

Majewski, A. R., Lynn, B. R., Lowdon, M. K., Williams, W. J., and Reist, J. D. 2013. Community composition of demersal marine fishes on the Canadian Beaufort Shelf and at Herschel Island, Yukon Territory. Journal of Marine Systems, 127: 55–64. https://doi.org/10.1016/j.jmarsys.2013.05.012.

Mantoura, R. F. C., and Woodward, E. M. S. 1983. Optimization of the indophenol blue method for the automated determination of ammonia in estuarine waters. Estuarine, Coastal and Shelf Science, 17: 219–224.

Marsh, J. M., Mueter, F. J., and Quinn, T. J. 2020. Environmental and biological influences on the distribution and population dynamics of polar cod (*Boreogadus saida*) in the US Chukchi Sea. Polar Biology, 43. https:/doi.org/10.1007/s00300-019-02561-w.

Mecklenburg, C. W., Mecklenburg, T. A., and Thorsteinson, L. K. 2002. Fishes of Alaska. American Fisheries Society, Bethesda, MD.

Melnikov, I. A., and Chernova, N. V. 2013. Characteristics of under-ice swarming of polar cod *Boreogadus saida* (Gadidae) in the Central Arctic Ocean. Journal of Ichthyology, 53: 7–15.

Mueter, F. J., Iken, K., Cooper, L. W., Grebmeier, J. M., Kuletz, K. J., Hopcroft, R. R., Danielson, S. L., *et al.* 2021. Changes in diversity and species composition across multiple assemblages in the eastern Chukchi Sea during two contrasting years are consistent with borealization. Oceanography, 34: 38–51. https://doi.org/10.5670/oceanog.2021.213.

Nelson, R. J., Bouchard, C., Fortier, L., Majewski, A. R., Reist, J. D., Præbel, K., Madsen, M. L., *et al.* 2020. Circumpolar genetic population structure of polar cod, *Boreogadus saida*. Polar Biology. https://doi.org/10.1007/s00300-020-02660-z.

Parker-Stetter, S. L., Horne, J. K., and Weingartner, T. J. 2011. Distribution of polar cod and age-0 fish in the U.S. Beaufort Sea. Polar Biology, 34: 1543–1557.

Parsons, T. R., Maita, Y., and Lalli, C. M. 1984. A manual of chemical and biological methods for seawater analysis. Pergamon Press, Oxford, UK, 173 pp.

Pinchuk, A. I., and Eisner, L. B. 2017. Spatial heterogeneity in zooplankton summer distribution in the eastern Chukchi Sea in 2012-2013 as a result of large-scale interactions of water masses. Deep Sea Research Part II: Topical Studies in Oceanography, 135: 27–39. https://doi.org/10.1016/j.dsr2.2016.11.003.

Pritchard, J. K., Stephens, M., and Donnelly, P. 2000. Inference of population structure using multilocus genotype data. Genetics, 155: 945–959. https://doi.org/10.1093/genetics/155.2.945.

Ratnasingham, S., and Hebert, P. D. N. 2007. bold: The Barcode of Life Data System (http://www.barcodinglife.org). Molecular Ecology Notes, 7: 355–364. https://doi.org/10.1111/j.1471-8286.2007.01678.x.

Ryan, T. E., Downie, R. A., Kloser, R. J., and Keith, G. 2015. Reducing bias due to noise and attenuation in open-ocean echo integration data. ICES Journal of Marine Science, 72: 2482–2493. https://doi.org/10.1093/icesjms/fsv121.

Simmonds, J., and MacLenna, D. N. 2006. Fisheries Acoustics: Theory and Practice. Wiley-Blackwell, Oxford, UK, 472 pp.

Søreide, J. E., Hop, H., Carroll, M. L., Falk-Petersen, S., and Hegseth, E. N. 2006. Seasonal food web structures and sympagic–pelagic coupling in the European Arctic revealed by stable isotopes and a two-source food web model. Progress in Oceanography, 71: 59–87.

Søreide, J. E., Leu, E. V. A., Berge, J., Graeve, M., and Falk-Petersen, S. 2010. Timing of blooms, algal food quality and Calanus glacialis reproduction and growth in a changing Arctic. Global Change Biology, 16: 3154–3163. https://doi.org/10.1111/j.1365-2486.2010.02175.x

Timco, G. W., and Frederking, R. M. W. 1996. A review of sea ice density. Cold Regions Science and Technology, 24: 1–6. https://www.sciencedirect.com/science/article/pii/0165232X9500007X.

Timmermans, M. -L., and Labe, Z. M. 2022. Sea surface temperature. pp. 41-47 *In* Arctic Report Card 2021. Edited by M. L. Druckenmiller, R. L. Thoman, and T. A. Moon. National Oceanic and Atmospheric Administration, Washington, DC. https://doi.org/10.25923/2y8r-0e49.

Urmy, S. S., Horne, J. K., and Barbee, D. H. 2012. Measuring the vertical distributional variability of pelagic fauna in Monterey Bay. ICES Journal of Marine Science, 69: 184–196. https://doi.org/10.1093/icesjms/fsr205.

van Franeker, J. A., Flores, H., and Van Dorssen, M. 2009. The Surface and Under Ice Trawl (SUIT). Ph.D. thesis, University of Groningen, pp. 181–188 *In* Frozen Desert Alive - The Role of Sea Ice for Pelagic Macrofauna and its Predators. Edited by H. Flores. Ponsen & Looijen,Wageningen, NL.

Vestfals, C. D., Mueter, F. J., Hedstrom, K. S., Laurel, B. J., Petrik, C. M., Duffy-Anderson, J. T., and Danielson, S. L. 2021. Modeling the dispersal of polar cod (*Boreogadus saida*) and saffron cod (*Eleginus gracilis*) early life stages in the Pacific Arctic using a biophysical transport model. Progress in Oceanography, 196: 102571. https://doi.org/10.1016/j.pocean.2021.102571.

Wang, S. W., Budge, S. M., Gradinger, R. R., Iken, K., and Wooller, M. J. 2014. Fatty acid and stable isotope characteristics of sea ice and pelagic particulate organic matter in the Bering Sea: tools for estimating sea ice algal contribution to Arctic food web production. Oecologia, 174: 699–712. https://doi.org/10.1007/s00442-013-2832-3.

Weingartner, T. J., Pickart, R., Winsor, P., Corlett, W. B., Dobbins, E. L., Fang, Y.-C., Irvine, C., *et al.* 2017. Characterization of the circulation on the continental shelf areas of the northeast Chukchi and western Beaufort seas. OCS Study BOEM 2017-065, U.S. Department of the Interior, Bureau of Ocean Energy Management, Alaska OCS Region, 221 pp.

Wilson, R. E., Sage, G. K., Wedemeyer, K., Sonsthagen, S. A., Menning, D. M., Gravley, M. C., Sexson, M. G., *et al.* 2019. Micro-geographic population genetic structure within Arctic cod (*Boreogadus saida*) in Beaufort Sea of Alaska. ICES Journal of Marine Science, 76: 1713–1721. https://doi.org/10.1093/icesjms/fsz041.

Wilson, R. E., Sonsthagen, S. A., Smé, N., Gharrett, A. J., Majewski, A. R., Wedemeyer, K., Nelson, R. J., *et al.* 2020. Mitochondrial genome diversity and population mitogenomics of polar cod (*Boreogadus saida*) and Arctic dwelling gadoids. Polar Biology, 43: 979–994. https://doi.org/10.1007/s00300-020-02703-5

Zong, F., Zhang, S., Chen, P., Yang, L., Shao, Q., Zhao, J., and Wei, L. 2022. Evaluation of sea ice concentration data using dual-polarized ratio algorithm in comparison with other satellite passive microwave sea ice concentration data sets and ship-based visual observations. Frontiers in Environmental Science, 10: 856289. https://doi.org/10.3389/fenvs.2022.856289.

Zuur, A. F., Saveliev, A. A., and Ieno, E. N. 2012. Zero Inflated Models and Generalized Linear Mixed Models with R. Highland Statistics Limited, Newburgh, UK, 334 pp.

APPENDICES

Appendix 1: CTD profiles

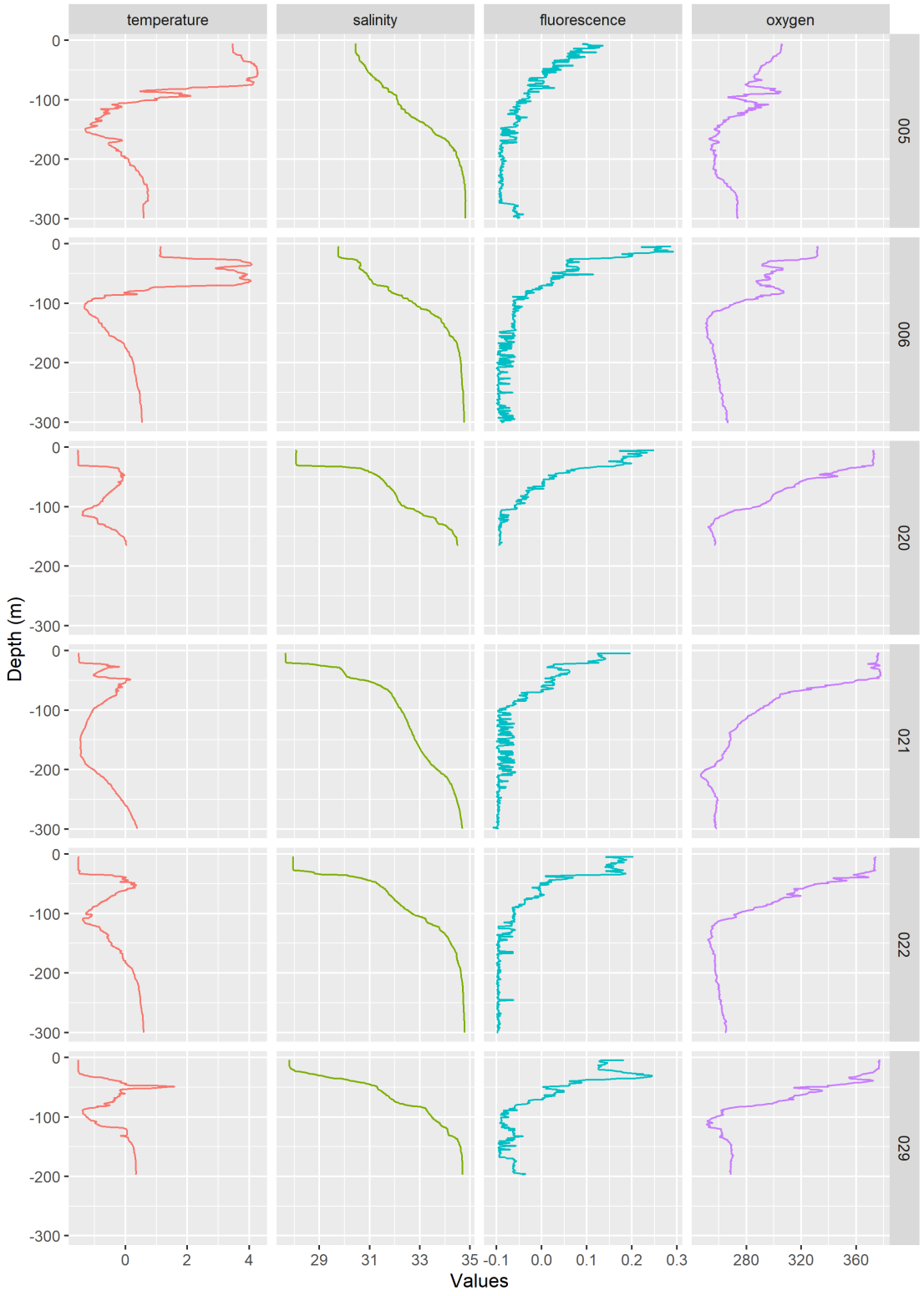

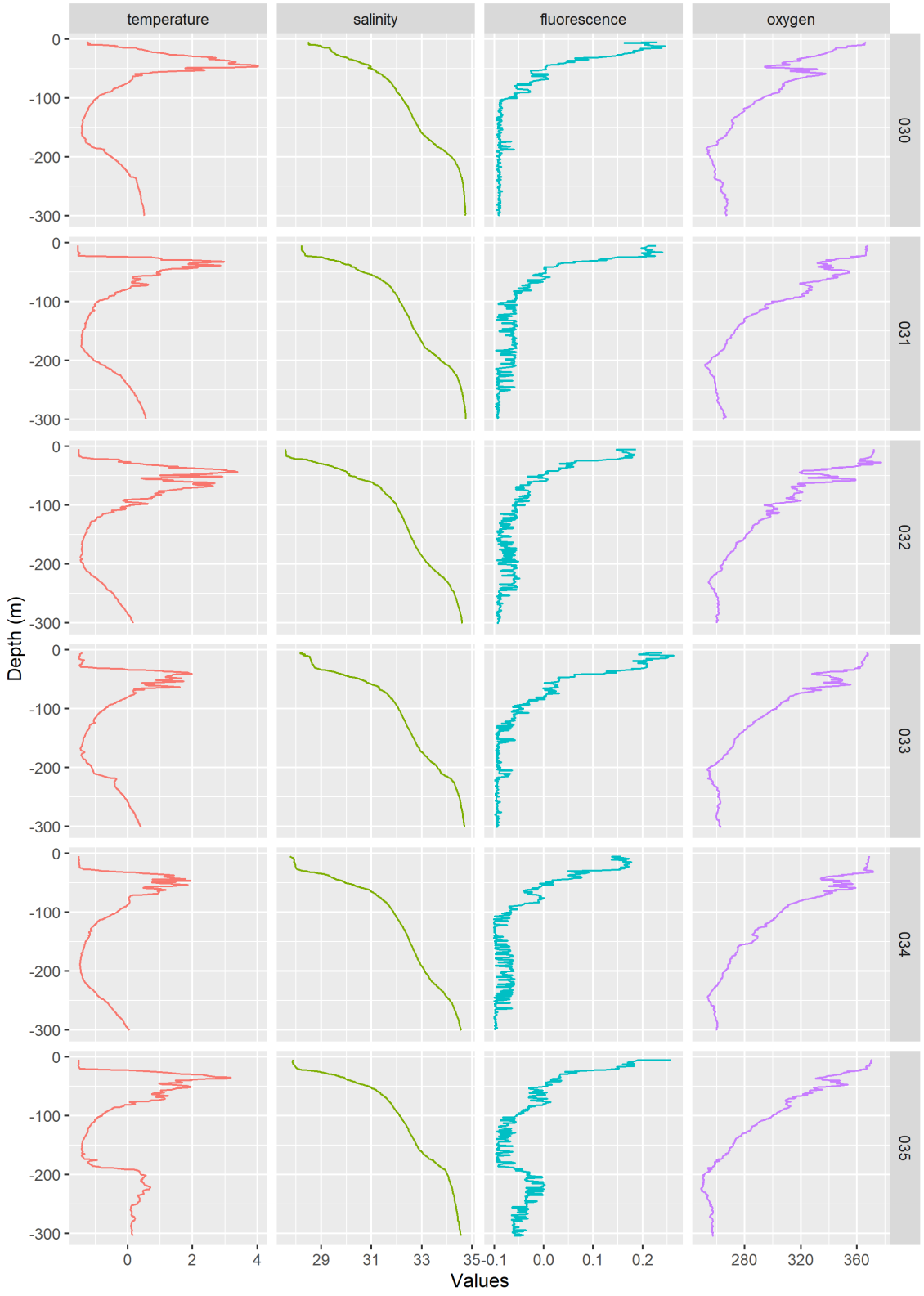

Figure A1: CTD profiles of temperature, salinity, chlorophyll fluorescence, and oxygen at each oceanographic sampling station (rows). See Figure 1 for station locations.

Appendix 2: Fish samples

Table A1: List of all fish sampled by Methot trawl and by Surface and Under-Ice Trawl (SUIT, in either fish or plankton net) by station and species with individual total length (TL, cm), standard length (mm), weight (g) and eviscerated weight (g, after removing stomach and gut).

Station	Gear	Net	Taxon	TL	SL	Weight	Evisc W
006	Methot		Ammodytes hexapterus	7.2		0.8	
006	Methot		Arctogadus glacialis	4.6	40	0.45	
006	Methot		Boreogadus saida	6.7	56	1.65	1.3
006	Methot		Boreogadus saida	7.55	68	2.35	1.95
006	Methot		Boreogadus saida	7.8	66	2.65	1.95
006	Methot		Boreogadus saida	6	49	1.15	0.85
006	Methot		Boreogadus saida	6.6	57	1.7	1.25
006	Methot		Boreogadus saida	8	66	2.7	2.15
006	Methot		Boreogadus saida	6.4	53	1.45	1
006	Methot		Boreogadus saida	6.4	53	2.2	1.9
006	Methot		Boreogadus saida	10.8	90	6.65	5.35
006	Methot		Boreogadus saida	6.5	54	1.5	1
006	Methot		Boreogadus saida	7.5	63	2.25	1.85
006	Methot		Boreogadus saida	5.6	45	0.9	0.65
006	Methot		Boreogadus saida	7.7	65	2.15	1.8
006	Methot		Boreogadus saida	8.1	66	2.7	2.01
006	Methot		Boreogadus saida	7.2	60	1.85	1.5
006	Methot		Boreogadus saida	7.7	65	2.4	2.05
006	Methot		Boreogadus saida	6.1	50	1.2	0.8
006	SUIT	Fish	Ammodytes hexapterus	9.6	88	1.8	
006	SUIT	Fish	Boreogadus saida	8	73	2.5	
006	SUIT	Fish	Threespined stickleback	4.9	43	0.7	
006	SUIT	Fish	Threespined stickleback	4.3	38	0.4	
006	SUIT	Fish	Threespined stickleback	4.3	37	0.6	
006	SUIT	Fish	Threespined stickleback	4.1	35	0.5	
006	SUIT	Fish	Threespined stickleback	4.8	42	0.8	
020	SUIT	Fish	Arctogadus glacialis	4.7	4	0.55	
020	SUIT	Fish	Arctogadus glacialis	4.4	3.9	0.4	
020	SUIT	Fish	Arctogadus glacialis	4.3	3.9	0.35	
020	SUIT	Fish	Boreogadus saida	8.1	6.9	2.95	2.2
020	SUIT	Fish	Boreogadus saida	6.1	5	1.15	0.75
020	SUIT	Fish	Boreogadus saida	6.6	5.5	1.5	0.85
020	SUIT	Fish	Boreogadus saida	5.8	4.9	1.25	0.6
020	SUIT	Fish	Boreogadus saida	7.8	6.7	2.95	
020	SUIT	Fish	Boreogadus saida	7.2	5.4	1.35	0.85
021	SUIT	Fish	Boreogadus saida	8.9	7.5	4.6	3.35
021	SUIT	Fish	Boreogadus saida	7.6	6.5	2.3	1.85

Station	Gear	Net	Taxon	TL	SL	Weight	Evisc W
021	SUIT	Fish	Boreogadus saida	8	6.6	3.2	2.45
021	SUIT	Fish	Boreogadus saida	7	6	2.15	1.8
021	SUIT	Fish	Boreogadus saida	10.2	8.6	6.25	5.45
021	SUIT	Fish	Boreogadus saida	6.3	5.2	1.5	1.1
021	SUIT	Fish	Boreogadus saida	7.1	6	2.2	1.25
021	SUIT	Fish	Boreogadus saida	6.2	5	1.45	1
021	SUIT	Fish	Boreogadus saida	9	7.5	3.95	3.05
021	SUIT	Fish	Boreogadus saida	7.2	6.1	1.85	
021	SUIT	Fish	Boreogadus saida	6.3	5.5	1.7	
021	SUIT	Fish	Boreogadus saida	5.9	5	1.3	
021	SUIT	Plankton	Boreogadus saida	8.2	7	3.15	2.8
021	SUIT	Fish	Boreogadus saida	5.2	4.4	0.9	
021	SUIT	Fish	Boreogadus saida	7.7	6.8	3.1	2.35
021	SUIT	Fish	Boreogadus saida	7.7	6.4	2.85	1.95
021	SUIT	Fish	Boreogadus saida	6.2	5.3	1.3	
021	SUIT	Fish	Boreogadus saida	8.3	7	4.6	2.7
021	SUIT	Fish	Boreogadus saida	14.2	11.9	17.25	13.13
021	SUIT	Fish	Boreogadus saida	6.2	5.2	1.25	0.9
021	SUIT	Fish	Boreogadus saida	6.7	5.5	1.55	1.15
021	SUIT	Fish	Boreogadus saida	9.5	7.8	5.8	4.4
021	SUIT	Fish	Boreogadus saida	9	7.4	4.45	3.25
021	SUIT	Fish	Boreogadus saida	9.5	8.2	4.45	3.45
021	SUIT	Fish	Boreogadus saida	8.3	6.9	3.25	2.45
021	SUIT	Fish	Boreogadus saida	8.7	7.2	3.95	3.05
021	SUIT	Fish	Boreogadus saida	9.6	8	5.65	4.25
021	SUIT	Fish	Boreogadus saida	7	5.8	1.65	1.15
021	SUIT	Fish	Boreogadus saida	7.6	6.2	2.1	1.35
021	SUIT	Fish	Boreogadus saida	6.9	5.5	1.75	1.25
021	SUIT	Fish	Boreogadus saida	8.5	7.1	3.65	2.65
022	SUIT	Fish	Boreogadus saida	8.3	7.1	3.35	2.3
022	SUIT	Fish	Boreogadus saida	8	6.6	2.85	2.4
022	SUIT	Fish	Boreogadus saida	5.1	4.4	2.85	2.4
022	SUIT	Fish	Boreogadus saida	6.2	5.2	1.3	0.9
022	SUIT	Fish	Boreogadus saida	7.1	6.2	2.15	1.55
022	SUIT	Fish	Boreogadus saida	7.1	6	1.7	1.35
022	SUIT	Fish	Boreogadus saida	8.1	7	2.6	2.2
029	SUIT	Fish	Boreogadus saida	6.5	5.7	1.5	1.2
029	SUIT	Plankton	Boreogadus saida	7.6	6.5	2.05	1.55
030	SUIT	Fish	Boreogadus saida	7.8	6.6	2.5	1.9
030	SUIT	Fish	Boreogadus saida	7	5.8	1.8	
030	SUIT	Fish	Boreogadus saida	7.2	6.2	2	

Station	Gear	Net	Taxon	TL	SL	Weight	Evisc W
030	SUIT	Fish	Boreogadus saida	7.2	6.2	2	
030	SUIT	Fish	Boreogadus saida	6.7	5.6	1.8	
030	SUIT	Fish	Boreogadus saida	6.5	5.5	1.3	
030	SUIT	Fish	Boreogadus saida	8	6.6	2.7	2.1
030	SUIT	Fish	Boreogadus saida	6.8	5.7	1.65	1.4
030	SUIT	Plankton	Boreogadus saida	8.3	7	2.9	2.3
030	SUIT	Fish	Boreogadus saida	8.2	6.9	2.85	2
030	SUIT	Fish	Boreogadus saida	7.8	7.2	2.55	2.15
030	SUIT	Fish	Boreogadus saida	6.7	57	1.5	
030	SUIT	Fish	Boreogadus saida	9.1	8.4	4.1	3.5
030	SUIT	Fish	Boreogadus saida	7.2	5.5	1.3	
030	SUIT	Fish	Boreogadus saida	7.6	6.5	2.55	2
030	SUIT	Fish	Boreogadus saida	7.4	6.9	2.5	2
030	SUIT	Fish	Boreogadus saida	6.6	5.5	1.55	1.25
030	SUIT	Fish	Boreogadus saida	8.4	7.2	1.85	1.6
030	SUIT	Fish	Boreogadus saida	7.1	6.7	1.9	1.65
030	SUIT	Fish	Boreogadus saida	7.8	6.5	2.35	2
030	SUIT	Fish	Boreogadus saida	8	7.5	2.9	2.35
030	SUIT	Fish	Boreogadus saida	8.2	7.1	2.95	2.5
030	SUIT	Plankton	Boreogadus saida	6.8	5.8	2.1	1.55
030	SUIT	Fish	Boreogadus saida	6.4	6	1.45	1.25
030	SUIT	Fish	Boreogadus saida	7	6.6	1.85	1.6
030	SUIT	Fish	Boreogadus saida	8.2	6.1	2.6	2.3
030	SUIT	Fish	Boreogadus saida	7.1	6.6	1.65	1.45
030	SUIT	Fish	Boreogadus saida	7.1	6	1.85	1.6
030	SUIT	Fish	Boreogadus saida	7.7	6.4	2.3	
030	SUIT	Fish	Boreogadus saida	7.1	6.1	1.95	1.65
030	SUIT	Fish	Boreogadus saida	7.2	6.1	2.2	1.85
030	SUIT	Fish	Boreogadus saida	7.7	6	1.9	
030	SUIT	Fish	Boreogadus saida	7.9	7.1	2.3	
030	SUIT	Fish	Boreogadus saida	8.3	7.2	3.25	1.15
030	SUIT	Fish	Boreogadus saida	6.8	5.7		
030	SUIT	Fish	Boreogadus saida	7.7	6.4	2.7	
030	SUIT	Fish	Boreogadus saida	6.7	6.2	2.75	1.4
031	SUIT	Fish	Boreogadus saida	7.2	6	2	
031	SUIT	Fish	Boreogadus saida	7.6	6.3	2.5	1.9
031	SUIT	Fish	Boreogadus saida	8	7.7	3.55	3.05
031	SUIT	Fish	Boreogadus saida	9	7.8	4.45	
031	SUIT	Fish	Boreogadus saida	10.6	9	6.4	5.2
031	SUIT	Fish	Boreogadus saida	7.8	6.6	2.9	
031	SUIT	Fish	Boreogadus saida	7.6	6.4	2.4	1.95

Station	Gear	Net	Taxon	TL	SL	Weight	Evisc W
031	SUIT	Fish	Boreogadus saida			1.25	
031	SUIT	Fish	Boreogadus saida	7.2	6.3	2.1	
031	SUIT	Fish	Boreogadus saida	6.5	5.8	1.6	
031	SUIT	Fish	Boreogadus saida	6.7	5.7	1.5	
031	SUIT	Fish	Boreogadus saida	6.6	5.5	1.35	
031	SUIT	Fish	Boreogadus saida	7.8	6.5	2.55	
031	SUIT	Fish	Boreogadus saida	7.1	5.9	2.05	
031	SUIT	Fish	Boreogadus saida	7.8	6.3	2.6	1.9
031	SUIT	Fish	Boreogadus saida	7.7	6.5	2.25	1.95
031	SUIT	Fish	Boreogadus saida	7.5	6.3	2.55	1.6
032	SUIT	Fish	Boreogadus saida	7.3	6.1	2.35	1.8
032	SUIT	Fish	Boreogadus saida	8	6.6	2.65	2.15
032	SUIT	Fish	Boreogadus saida	7.6	6.5	2.6	1.85
032	SUIT	Fish	Boreogadus saida	8.1	6.7	3.15	2.45
032	SUIT	Fish	Boreogadus saida	7.6	6.5	2.4	1.95
032	SUIT	Fish	Boreogadus saida	7.6	6.3	2.5	2.15
033	SUIT	Fish	Boreogadus saida	7.4	6	2.1	1.5
033	SUIT	Fish	Boreogadus saida	8.2	6.7	2.95	2.25
034	SUIT	Fish	Boreogadus saida	7.5	6.2	2.85	
034	SUIT	Fish	Boreogadus saida	11.2	9.3	7.35	5.9
034	SUIT	Plankton	Boreogadus saida	7.3	6.1	2.15	1.5
034	SUIT	Fish	Boreogadus saida	7.1	5.9	2.15	
034	SUIT	Fish	Boreogadus saida	7.1	5.9	2.15	
034	SUIT	Fish	Boreogadus saida	6.3	5.2	1.6	
034	SUIT	Fish	Boreogadus saida	9.1	7.7	4.35	
034	SUIT	Plankton	Boreogadus saida	7.5	6.3	2.55	2.1
034	SUIT	Fish	Boreogadus saida	8.2	6.8	2.95	
034	SUIT	Fish	Boreogadus saida	6.4	5.2	1.6	
034	SUIT	Fish	Boreogadus saida	7.4	6	2.05	
034	SUIT	Fish	Boreogadus saida	7.4	6.2	1.9	
034	SUIT	Fish	Boreogadus saida	6.5	5.5	1.3	
034	SUIT	Fish	Boreogadus saida	6	4.9	1.05	
034	SUIT	Fish	Boreogadus saida	6.1	5.1	1.1	
034	SUIT	Fish	Boreogadus saida	6.7	5.5	1.5	
034	SUIT	Fish	Boreogadus saida	6.2	5.1	0.95	
034	SUIT	Fish	Boreogadus saida	6.1	5.2	1.05	
034	SUIT	Fish	Boreogadus saida	9.5	7.8	4.2	3.15
034	SUIT	Fish	Boreogadus saida	5.9	4.7	1	
034	SUIT	Fish	Boreogadus saida	6.1	4.9	1	
035	SUIT	Fish	Boreogadus saida	7.5	6.1	1.85	
035	SUIT	Fish	Boreogadus saida	8.8	7.4	3.15	

Station	Gear	Net	Taxon	TL	SL	Weight	Evisc W
035	SUIT	Plankton	Boreogadus saida	8.2	6.8	3	2.1
035	SUIT	Fish	Boreogadus saida	9.3	7.6	4.5	3.7
035	SUIT	Fish	Boreogadus saida	9	7.5	3.3	4.2
035	SUIT	Fish	Boreogadus saida	8.6	7.2	3.4	
035	SUIT	Fish	Boreogadus saida	8	6.6	2.55	
035	SUIT	Fish	Boreogadus saida	7.4	6.4	2.15	
035	SUIT	Fish	Boreogadus saida	7.1	5.8	1.65	
035	SUIT	Fish	Boreogadus saida	7.3	6	1.95	
035	SUIT	Fish	Boreogadus saida	7.3	6.1	2.15	
035	SUIT	Fish	Boreogadus saida	7.7	6.2	3.5	
035	SUIT	Fish	Boreogadus saida	8.6	7	3.5	
035	SUIT	Fish	Boreogadus saida	6.9	5.6	1.65	
035	SUIT	Fish	Boreogadus saida	7.3	6.1	2	
035	SUIT	Fish	Boreogadus saida	7.3	5.9	1.95	
035	SUIT	Fish	Boreogadus saida	7.2	6	1.9	
035	SUIT	Fish	Boreogadus saida	7.1	6	2.15	
035	SUIT	Fish	Boreogadus saida	8.1	6.6	2.7	

The Department of the Interior Mission

As the Nation’s principal conservation agency, the Department of the Interior has responsibility for most of our nationally owned public lands and natural resources. This includes fostering the sound use of our land and water resources, protecting our fish, wildlife and biological diversity; preserving the environmental and cultural values of our national parks and historical places; and providing for the enjoyment of life through outdoor recreation.The Department assesses our energy and mineral resources andworks to ensure that their development is in the best interests of all our people by encouraging stewardship and citizen participation in their care. The Department also has a major responsibility for American Indian reservation communities and for people who live in island communities.

The Bureau of Ocean Energy Management

The Bureau of Ocean Energy Management (BOEM) works to manage the exploration and development of the nation's offshore resources in a way that appropriately balances economic development, energy independence, and environmental protection through oil and gas leases, renewable energy development and environmental reviews and studies.